

POLITECNICO DI TORINO

Corso di Laurea Magistrale
in INGEGNERIA DELL'AUTOVEICOLO

Tesi di Laurea Magistrale

**Modelling and Control of Non-Glare Zone Width of
Adaptive Driving Beam (ADB) in Different Driving
Scenarios**



Relatore
prof. Guido Albertengo

Candidato
Yihong Chen

2021 Ottobre

DECLARATION OF PREVIOUS PUBLICATION

I. Previous Publication

This thesis includes one original papers that have been previously submitted to journals for publication, as follows:

Thesis Chapter	Publication title/full citation	Publication status*
Chapter [1-4]	Optimizing Non-glare Zone Width of Adaptive Driving Beam (ADB) using Fuzzy Logic Control, <i>Applied Sciences</i> , 2021	<i>Accepted</i>

I certify that I have obtained a written permission from the copyright owner(s) to include the above published material(s) in my thesis. I certify that the above material describes work completed during my registration as a graduate student at the University of Windsor.

II. General

I declare that, to the best of my knowledge, my thesis does not infringe upon anyone's copyright nor violate any proprietary rights and that any ideas, techniques, quotations, or any other material from the work of other people included in my thesis, published or otherwise, are fully acknowledged in accordance with the standard referencing practices. Furthermore, to the extent that I have included copyrighted material that surpasses the bounds of fair dealing within the meaning of the Canada Copyright Act, I certify that I have obtained a written permission from the copyright owner(s) to include such material(s) in my thesis.

I declare that this is a true copy of my thesis, including any final revisions, as approved by my thesis committee and the Graduate Studies office, and that this thesis has not been submitted for a higher degree to any other University or Institution.

ABSTRACT

Adaptive driving beam (ADB) is an advanced vehicle forward lighting system that automatically adapts its beam patterns to create a non-glare zone around vehicles, providing good long-range visibility for the driver without causing an uncomfortable glare for other road users. The performance of the ADB system is affected by the non-glare zone width. A narrow non-glare zone could create indirect glare in the side rear-view mirrors of preceding vehicles during sharp turns, while widening it results in poor road illumination. This research studies the trade-off relationship between glare and road illumination when altering the width of the non-glare zone in different driving scenarios. The study is conducted by using virtual driving simulation tools to simulate an ADB vehicle on four S-curve roads with minimum curvatures varying from 25 m to 100 m. Lux data are collected and processed using a fuzzy logic controller to mimic a human test driver to find the best non-glare zone width for balancing the trade-off. The research developed a design methodology allowing for a better understanding of the effect adjusting the width of the ADB non-glare zone has on ADB performance and improved ADB non-glare zone width optimum control system design.

DEDICATION

To my father Chen Xiaojian, for everything

ACKNOWLEDGEMENTS

I would like to acknowledge the following people/organizations for their assistance in the completion of this thesis:

The University of Windsor, Politecnico di Torino, and Stellantis N.V. for providing such a unique dual international master program;

Prof. Jennifer Johrendt, Prof. Giovanni Belingardi, Prof.ssa Maria Pia Cavatorta, Marie Mills, and Edoardo Rabino, the program coordinators from all parties who have done an amazing job organizing the program;

Prof. Jalal Ahamed and Prof. Arash Ahmad from the University of Windsor, and Prof. Guido Albertengo from Politecnico di Torino, who are the academic advisors of the program, for academic support and guidance throughout the research;

Dennis Novack and Davide Secchiero, the industrial advisors of the program from Stellantis N.V., Sida Li, and Steven Simic, as well as the Automotive Research and Develop Center (ARDC) in Windsor, Ontario, for the guidance and support regarding the knowledge of vehicle lighting systems and their help in establishing the research topic;

Carsten Werner and the LucidDrive team from Synopsys GmbH for supporting the software.

Prof. Jennifer Johrendt and Prof. Shahpour Alirezaee, the committee members, for their time, valuable comments, and suggestions;

MITACS and Stellantis N.V. for financial support.

TABLE OF CONTENTS

DECLARATION OF PREVIOUS PUBLICATION.....	iii
ABSTRACT.....	v
DEDICATION.....	vi
ACKNOWLEDGEMENTS.....	vii
LIST OF TABLES.....	x
LIST OF FIGURES.....	xi
LIST OF ABBREVIATIONS/SYMBOLS.....	xiv
CHAPTER 1 INTRODUCTION.....	1
1.1. Background.....	1
1.2. Literature Review.....	4
1.3. Objective and Scope.....	10
CHAPTER 2 NIGHT DRIVE SIMULATOR.....	11
2.1. LucidDrive AFS Plug-in.....	12
2.2. Modification of LucidDrive AFS Plug-in.....	17
2.3. Driving Scenario Design.....	24
2.4. Virtual Stimulus Vehicle and Light Sensor.....	30
CHAPTER 3 DATA COLLECTION AND POST-PROCESSING.....	33
3.1. Data Acquired from LucidDrive.....	33
3.2. Fuzzy Logic Controller.....	41
3.3. Result.....	50
CHAPTER 4 CONCLUSIONS AND FUTURE OPPORTUNITIES.....	53
4.1. Conclusions.....	53
4.2. Future Opportunities.....	56
4.2.1. Physical Test.....	56

4.2.2.	Other Optimization Possibilities	57
4.2.2.1.	Sensor Fusion	58
4.2.2.2.	Steering and Other Vehicle Dynamic Sensors	58
4.2.2.3.	Real-Time Optimization: Navigation Information + Distance Sensor	59
4.2.2.4.	Regional Optimization: Navigation Information Only	59
	REFERENCES/BIBLIOGRAPHY.....	61
	VITA AUCTORIS	66

LIST OF TABLES

Table 1. Parameters of the driving scenario	30
Table 2. Parameters of the unscaled membership functions, range 0-1	44
Table 3. Variable range of the membership functions	44
Table 4. Trial 1 iteration of four driving scenarios, using the fuzzy logic controller with linear membership function.....	46
Table 5. Trial 2 iteration of four driving scenarios, using the fuzzy logic controller with Gauss membership function	47
Table 6. Best non-glare zone width vs. minimum curvature of the S-curve in all four driving scenario simulations.....	51

LIST OF FIGURES

Figure 1. Example of the curvy road where indirect glare from side rearview mirror is experienced by the preceding driver.	4
Figure 2. Illustration of the components of an ADB system.	5
Figure 3. Illustration of ADB non-glare zone.	5
Figure 4. Vehicle recognition technology based on vehicle taillight.....	6
Figure 5. Illustration of the cause of the side rearview mirror glare issues due to the limitation of light-based vehicles' recognition technology.	8
Figure 6. Illustration of matrix beam script, showing that it switches off certain LEDs of the matrix headlamp to create the non-glare zone.....	13
Figure 7. Example of eight-element matrix LED in LucidDrive simulation.	14
Figure 8. Example of matrix LED in LucidDrive simulation where only one LED is switched on.....	14
Figure 9. The graphical effect of ADB using matrix beam script in the simulation.....	15
Figure 10. Illustration of pixel masking script.....	16
Figure 11. The graphic effect of ADB using pixel masking script in the simulation.....	17
Figure 12. Graphical effect of the three-dimensional boundary box is created for the stimulus vehicle to simulate the vehicle recognition of ADB.....	18
Figure 13. ISO 8855 vehicle coordinate system used in the simulation.	19
Figure 14. The three-dimensional boundary box of the stimulus vehicle,.....	19
Figure 15. The two-dimensional boundary box of the stimulus vehicle.....	20

Figure 16. A graphical comparison in the simulator between the original and the modified ADB simulation.....	21
Figure 17. Effect on glare when altering non-glare zone width.....	23
Figure 18. Effect on road illumination when altering non-glare zone width.	24
Figure 19. Curvature of the driving path of the vehicle driving on a track transition curve with a minimum curvature of 25 m.....	25
Figure 20. Lateral acceleration of the vehicle driving on a track transition curve with a minimum curvature of 25 m.....	26
Figure 21. Driving scenarios prepared for the virtual night drive data collection.....	29
Figure 22. The position of the virtual light sensor.....	31
Figure 23. Rear view of the stimulus vehicle and the position of the virtual lux meter in the simulation.	31
Figure 24. Lux reading of S-curve with 25 m curvature simulation at 100% non-glare zone width.....	34
Figure 25. S-curve with 25 m curvature simulation at 100% non-glare zone width.	35
Figure 26. Lux reading of S-curve with 25 m curvature simulation in different non-glare zone width.....	37
Figure 27. Total glare time vs. non-glare zone width for S-curve with 25 m curvature	37
Figure 28. Lux reading of S-curve with 50 m curvature simulation in different non-glare zone width.....	38
Figure 29. S-curve with 50 m curvature, total glare time vs. non-glare zone width.	38

Figure 30. Lux reading of S-curve with 75 m curvature simulation in different non-glare zone width.....	39
Figure 31. S-curve with 75 m curvature, total glare time vs. non-glare zone width.	39
Figure 32. Lux reading of S-curve with 100 m curvature simulation in different non-glare zone width.....	40
Figure 33. S-curve with 100 m curvature, total glare time vs. non-glare zone width.	40
Figure 34. Schematic show fuzzy logic controller block diagram.....	42
Figure 35. Membership function of fuzzy logic controller.....	45
Figure 36. The minimum curvature in the driving scenario vs. best non-glare zone width.....	52
Figure 37. The ideal non-glare zone width enlarging direction for minimizing the effect on road illumination.....	55
Figure 38. The overlap of the lux reading plot and the lateral acceleration plot, showing the time gap between glare and vehicle dynamic inputs..	59

LIST OF ABBREVIATIONS/SYMBOLS

AAA	American Automobile Association
AASHTO	American Association of State Highway and Transportation Officials
ACC	Adaptive Cruise Control
ADB	Adaptive Driving Beam
AFS	Adaptive Forward-Lighting System
CMVSS	Canadian Motor Vehicle Safety Standards
DPM	Deformable Part Model
ECE	Economic Commission for Europe
FMVSS	Federal Motor Vehicle Safety Standards
GPS	Global Positioning System
ISO	International Organization for Standardization
LED	Light-Emitting Diode
NHTSA	National Highway Traffic Safety Administration
NPRM	Notice of Proposed Rulemaking
OEM	Original Equipment Manufacturer

SAE	Society of Automotive Engineers
UNECE	United Nations Economic Commission for Europe
VCS	Vehicle Coordinates System

CHAPTER 1

INTRODUCTION

This chapter will discuss the importance of automotive forward lighting and introduce the Adaptive Driving Beam (ADB) system by defining ADB, outlining the working principles behind ADB and its current state-of-the-art iterations, and introducing the homologation status of ADB in North America through literature review. Finally, the chapter details the issue that this research is targeting to solve.

1.1. Background

Automotive forward lighting is significant for driving safety, especially for night driving. Data from the National Highway Traffic Safety Administration (NHTSA) shows that the fatality rate associated with driving at night is approximately three times greater than traveling during the day [1]. An ideal forward-lighting system for vehicles should be able to provide adequate illumination of the road and surrounding area for the driver while not creating uncomfortable glares for other road users. Conventional vehicle forward-lighting systems have two fixed beam patterns: a high beam and a low beam. The high beam provides good long-range visibility to the driver but it will create strong glare for both oncoming and preceding vehicles. The low beam, however, minimizes the glare by sacrificing road illumination. Studies indicate that drivers seldom use high beams, mostly due to the concern of creating a discomforting glare for other road users [2][3][4]. A study from the American Automobile Association (AAA) suggests that, depending on the type of the lamp [5], the low beam only provides adequate illumination for speeds of 39 mph to 52 mph (63 km/h to 84 km/h), which is not sufficient for daily

driving. This concludes that there is a potential for the improvement of conventional vehicle forward-lighting systems regarding night driving safety. One of the latest technologies is ADB.

Adaptive Driving Beam (ADB) is an advanced vehicle forward-lighting system that automatically adapts its beam patterns to create a non-glare zone that includes both oncoming and preceding vehicles. Studies show that, in most driving scenarios, a vehicle equipped with ADB could provide the driver with road illumination equivalent to a high beam [6] while the glare it creates for other road users is similar to a vehicle with its low beam turned on [7][8].

ADB was first introduced in Europe in 2012, homologated by the United Nations Economic Commission for Europe (UNECE) R48 and R123 [9][10]. In North America, Canada was the first country to approve ADB by amendment of the Canadian Motor Vehicle Safety Standards (CMVSS) 108 [11]. At the time this thesis research was conducted, however, ADB was not homologated by the NHTSA in the United States; thus, vehicles that are currently being sold in the United States that can not be equipped with ADB. This is due to conflict with the NHTSA Federal Motor Vehicle Safety Standards (FMVSS) 108 [12], which specify the photometry requirements of high beams and low beams. Since the beam pattern of ADB changes dynamically, it cannot meet the photometry requirements of either high beams or low beams. ADB's homologation process in North American is currently progressing, however, since Toyota North America petitioned NHTSA in 2013 to amend the FMVSS 108 to allow ADB [13], which was later responded to by NHTSA in 2018 in the form of a Notice of Proposed Rulemaking (NPRM) [14], along with its own proposed ADB testing procedure. In 2016,

the Society of Automotive Engineers (SAE) published its recommended practices for ADB homologation [15], which was later adopted by Canadian legislation in 2018 for the purpose of ADB type approval testing [11]. It can be expected that ADB will be homologized by NHTSA in the near future; at that time, ADB will rise in popularity as more and more vehicles will be equipped with it. American automakers should invest in researching ADB and be ready to launch their ADB vehicles as soon as NHTSA's rulemaking process is complete.

The target of this research is to improve our understanding of better ADB tuning, which could be beneficial for automotive original equipment manufacturers (OEM) hoping to improve the ADB system for specific driving scenarios. It was observed that, when an ADB vehicle navigates some sharp corners, the driver of the vehicle in front of the ADB vehicle moving in the same direction would experience undesired glare from the side rearview mirror. An example of such a sharp corner is shown in Figure 1, where the minimum curvature of the pointed S-curve is approximately 25 m. The research will begin by understanding the cause behind this issue and reproducing it in a night drive simulator before finally proposing a solution to this glare issue.



©2021 Microsoft Corporation, ©2021 TomTom

Figure 1. Example of the curvy road where indirect glare from side rearview mirror is experienced by the preceding driver.

1.2. Literature Review

The current ADB system consists of three major components [16][17][18][19]: a vision-based camera that is able to recognize other vehicles on road, an electronic control unit that receives the camera's signal and manipulates the headlamp's LEDs (light-emitting diodes), and a pair of segment or matrix LED headlamps which can project different beam patterns, as shown in Figure 2. The performance of the ADB mainly depends on how well the system can recognize other road users and how accurately the headlight can project the non-glare zone. A segmental or pixel LED headlamp consists of multiple LEDs which can be switched on/off individually. When the signals of other vehicles are received from the camera, the specific LEDs will be switched off automatically to create a non-glare zone around other road users, while other regions remain at the high beam level of illumination, as illustrated in Figure 3. Segmental LED

can be considered a special type of pixel LED, with one row of LEDs in each lamp, while pixel LED has multiple rows, which could provide more precise control of the beam pattern.

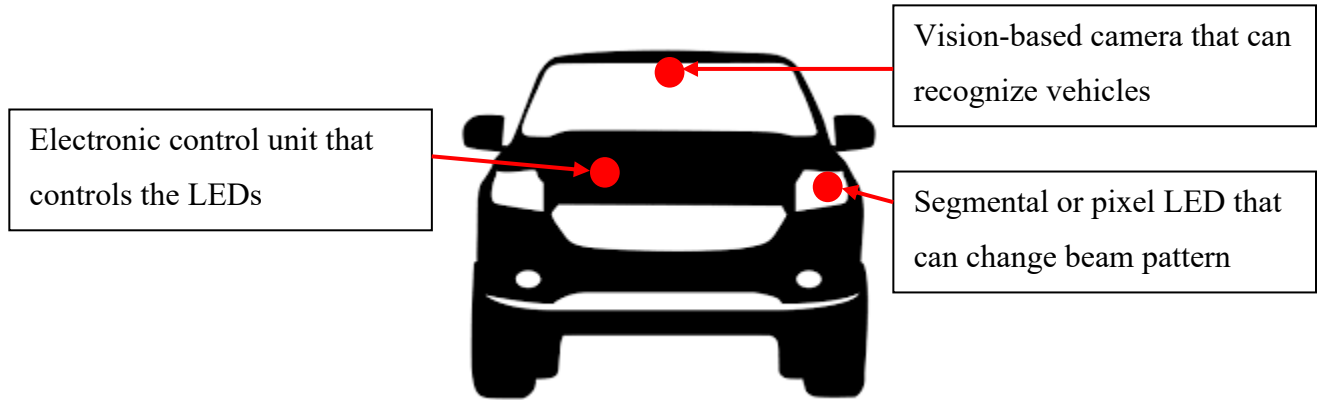


Figure 2. Illustration of the components of an ADB system.

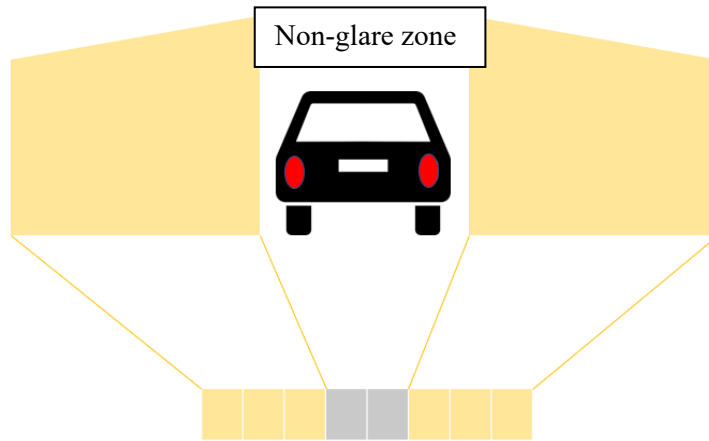


Figure 3. Illustration of ADB non-glare zone.

Luo Feng and Hu Fengjian [20] did a comprehensive survey of different types of vision-based adaptive forward-lighting system (AFS), finding that, although there are

multiple methods of vehicle recognition, due to poor lighting conditions at night, the camera in the ADB system recognizes vehicles by only the light projected from them instead of recognizing the entire geometry of the vehicle. This is also stated in the Valeo technical bulletin of ADB [19]. Most of the nighttime vehicle detection and recognition algorithms are based on the light's color [21][22][23] and symmetry [24][25], which differentiate the taillights of the vehicle from ambient lights. Figure 4 illustrates the vehicle recognition technology based on the vehicle's taillight, where a) is the original image taken from the camera, which is later processed into b), where the taillight is filtered out from the surroundings and a boundary box is created around the recognized taillights. Finally, in c), with the boundary box overlapping the original image, the position of the vehicle is highlighted by the system.

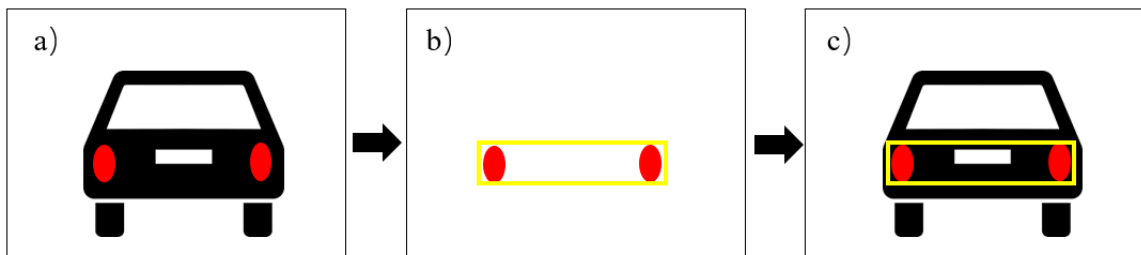


Figure 4. Vehicle recognition technology based on vehicle taillight, showing that the recognized boundary box is only based on the shape of the taillight instead of the entire geometry of the vehicle.

Such technology bypasses the difficulty of image recognition in poor lighting conditions, yet accurately delivers the position and location of the vehicles. For applications such as automatic high beams, in which the vehicle's lights automatically switch to low when other vehicles are detected, this technology would be sufficient. The technology also has a limitation, however, as the boundary box solely relies on vehicle's

lights, which do not accurately reflect the whole geometry of the vehicle. That is to say, if the vehicle is not straight while in front of the camera, but in a cornering maneuver, the boundary box would fail to cover the whole vehicle's geometry. Since the non-glare zone is created based on the boundary box recognized by the camera in an ADB application, when the side rearview mirror is excluded from the boundary box, glare will be experienced. Figure 5 provides the top view of a vehicle traveling in the same direction as an ADB vehicle, the red line represents the boundary box created by light-based vehicle recognition. The left image shows the situation of the vehicle, straightly positioned in front of the ADB vehicle, in which the non-glare zone successfully covers the entire vehicle. In the image on the right, however, which shows the vehicle cornering, the side rearview mirror will be exposed in the high beam area. That is the reason that glare from the side rearview mirror is experienced.

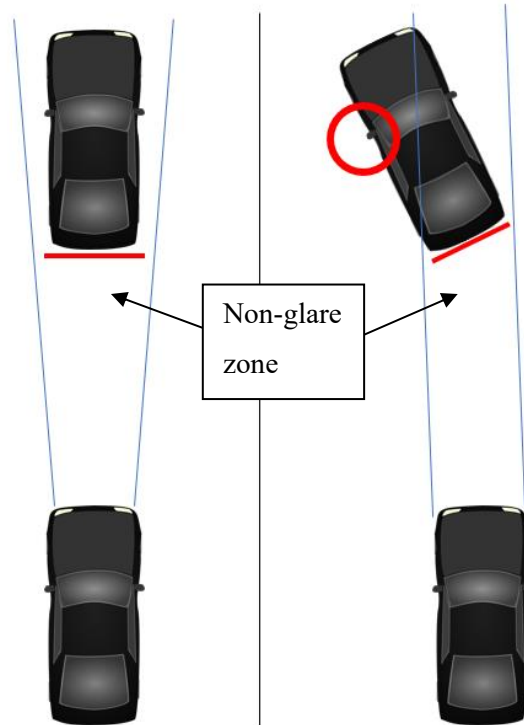


Figure 5. Illustration of the cause of the side rearview mirror glare issues due to the limitation of light-based vehicles' recognition technology, showing that, if the stimulus vehicle is not straightly aligned with the ADB vehicle, the side rearview mirror will be exposed in the non-glare zone.

There are several approaches to solving this issue, one of which is improving the vehicle recognition technology, allowing the system to create a boundary box around the true geometry of the vehicle, solving the issue fundamentally. Tehrani et al. [26] improved the performance for vehicle detection at night using a deformable part model (DPM) with a lateral filter that allows the system to recognize the vehicle geometry in low-lighting conditions. DPM was widely used for object recognition and was proved outstanding performance and accuracy in well-lighted conditions. Their team compared the results of urban night drive scenarios between normal deformable part models and the optimized model, showing there is a potential for using the improved model for night

vision applications, though further research should still be conducted. Zeng et al. [27] presented a vehicle recognition algorithm with low-light enhancement with artificial intelligence and machine learning. Balci et al. [28] proposed an approach for images captured at nighttime that uses near-infrared camera images with deep learning. Those algorithms show the potential of such detection being used for future ADB systems.

Another approach is using the same light-based vehicle recognition technology while introducing additional inputs to allow the system to predict the maneuvering of the stimulus vehicle. Götz et al. [29] improved the ADB system using sensor fusion and predictive algorithms in twisting roads and passing-car scenarios. In the field of adaptive forward-lighting systems (AFS), Gao and Li [30] studied eye-tracking technology and Bradai [31] presented a navigation-based virtual sensor for the AFS. Headlamps with AFS provide better road illumination during cornering by swiping the light into the corner. Conventionally, the input provided to the system is the steering angle and vehicle speed. Ideally, the headlamp should swipe as soon as the driver sees the corner but before steering, as using the steering angle as the input could introduce a slight delay to the response. Sensor fusion with eye-tracking technology or navigation could reduce such delay. For an ADB, the steering angle input is not ideal for sensor fusion, as the time gap between when the stimulus vehicle enters the corner and the ADB vehicle starts steering is long enough to create uncomfortable glare. Eye-tracking technology and navigation, however, could be more responsive and could also be applied to ADB. With those additional inputs, the system could adjust the non-glare zone accordingly, thus eliminating unwanted glares.

1.3. Objective and Scope

Each such improvement of ADB requires additional hardware for the system or a more advanced algorithm. With the currently existing system, this problem can also be solved by widening the non-glare zone, though at the cost of road illumination. The question is how to find the best non-glare zone width to balance the issue of glare and road illumination.

This research studies the trade-off relationship between road illumination and side rearview mirror glare, along with the influence of different road curvatures. The research aims to provide automakers with a guideline for the fine-tuning of the current ADB system by adjusting the non-glare zone width. The research is conducted on a virtual night drive simulator called LucidDrive and presents a proof of concept for using fuzzy logic control to mimics a human test driver in finding the best non-glare zone width.

The novelty of the research includes:

- Designing a night drive experiment to objectively study the trade-off relationship between glare and road illumination.
- Conducting the experiment and objective data collection in a virtual night drive environment, which is much more cost- and time-efficient compared to conventional physical night drives.
- Using a fuzzy logic controller to mimic human decisions to find the best non-glare zone width.

CHAPTER 2

NIGHT DRIVE SIMULATOR

This chapter discusses the methodology of this study, introducing the night drive simulator that was used to conduct the research, as well as the design of the experiment. Conventional physical tests of vehicle lighting systems can be categorized into outdoor and indoor tests, both of which have many restrictions and inconveniences. For outdoor tests, one of the most obvious inconvenience is the time of the test, which must be performed after sunset to best eliminate the effect of ambient light. For that reason, engineers and testers have to make special arrangements to perform the tests, especially in high latitude cities where the sunset comes late in the summer. Indoor testing facilities have better controls over the ambient environment, but, due to the limitations of facility size, they are mainly used to conduct static tests, which cannot be used for this research since the beam pattern of the ADB vehicles dynamically change during driving and also because the research is meant to study ADB performance during cornering. Additionally, due to the current legislation status of ADB in North America, access to ADB vehicles is limited. As a result, a virtual night drive simulator was preferred to perform this study.

Created by Synopsys, Inc., LucidDrive is a standalone night drive simulator that is designed to deliver a visual presentation of the vehicle headlight performance during driving. It allows engineers to intuitively evaluate the performance of the vehicle lighting system as if it were functioning during real-world driving. The default built-in AFS module allows it to simulate ADB function, making this software suitable for this research. There are still challenges, however, when it comes to using the software out-of-the-box:

- Default built-in ADB simulation module idealized ADB and, thus, could not realistically recreate the glare issue during cornering; and
- LucidDrive is designed for subjective evaluation but not for objective data collection.

These two challenges will be discussed in this chapter.

2.1. LucidDrive AFS Plug-in

The first step of the research is to reproduce the ADB system and the side rear-view mirror glare problem in the night drive simulator. The simulator provided two approaches for simulating the ADB function within the Adaptive Forward-Lighting System (AFS) plug-in of the software: pixel masking and matrix beam [32].

The matrix beam script simulates the operation of a real ADB control system, turning each single LED off and on to create the non-glare zone, as illustrated in Figure 6. This requires inputting the beam pattern file of each LED in the ADB lamps into the simulation. Shown in Figure 7 is an example of an eight-element segmental LED, which means that each lamp, left or right, consists of eight individual beam pattern files. Figure 8 shows the capability of switching on only one LED while others remain switched off. Acquiring those beam pattern files may be difficult – a detail that will be discussed in Chapter 4, the physical test of the future opportunities. Figure 9 shows the graphic effects of ADB using the matrix beam script in the simulation. The red square indicates the boundary box of the stimulus vehicle, and the virtual wall shows the instantaneous beam pattern of the lamp. It can be seen that the non-glare zone is created by switching off a few LEDs in both left and right lamps.

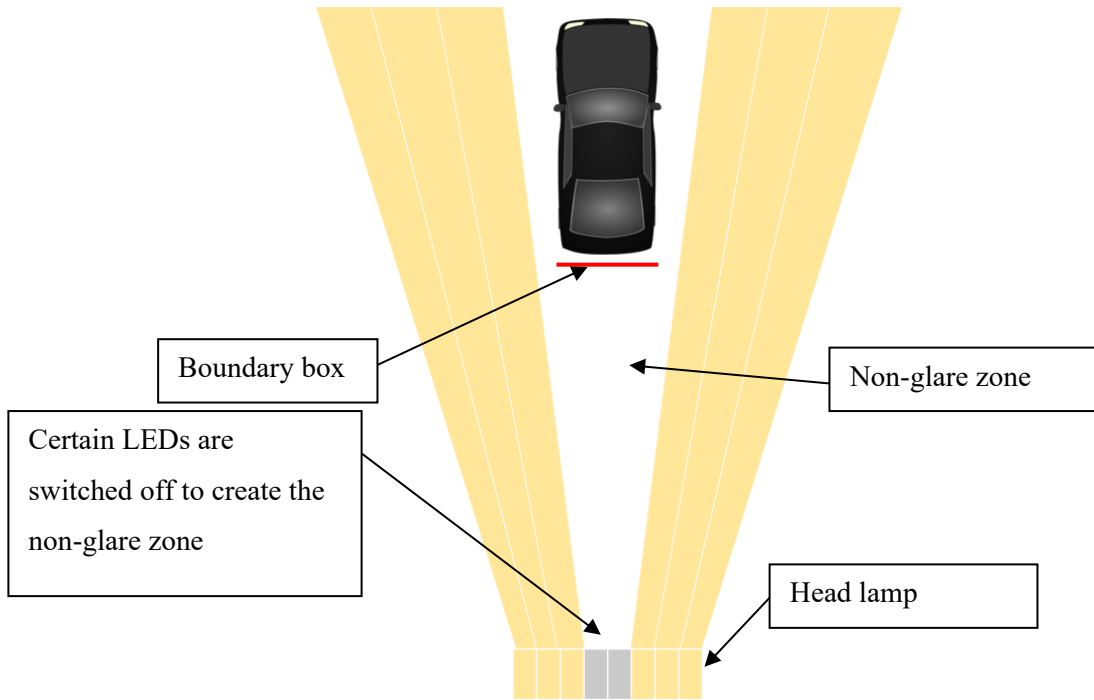


Figure 6. Illustration of matrix beam script, showing that it switches off certain LEDs of the matrix headlamp to create the non-glare zone.



Figure 7. Example of eight-element matrix LED in LucidDrive simulation.



Figure 8. Example of matrix LED in LucidDrive simulation where only one LED is switched on, showing that each LED can be switched on/off individually.



Figure 9. The graphical effect of ADB using matrix beam script in the simulation.

Pixel masking, on the other hand, creates a virtual mask in front of the lamp, shading out the non-glare zone according to the shape of the boundary box, as illustrated in Figure 10. It can be considered to be simulating ideal ADB lamps, as the non-glare zone is exactly the shape of the boundary box. This could be achieved by increasing the number of LEDs in the matrix beam. One benefit of using this script is that it does not require the beam pattern file of individual LEDs. In the event that the beam pattern file of the ADB lamp cannot be acquired, automotive OEMs can still scan the overall beam pattern of a production vehicle in a lab environment and use pixel masking to achieve the ADB simulation. The graphic effect of ADB using the pixel masking script in the simulation is shown in Figure 11.

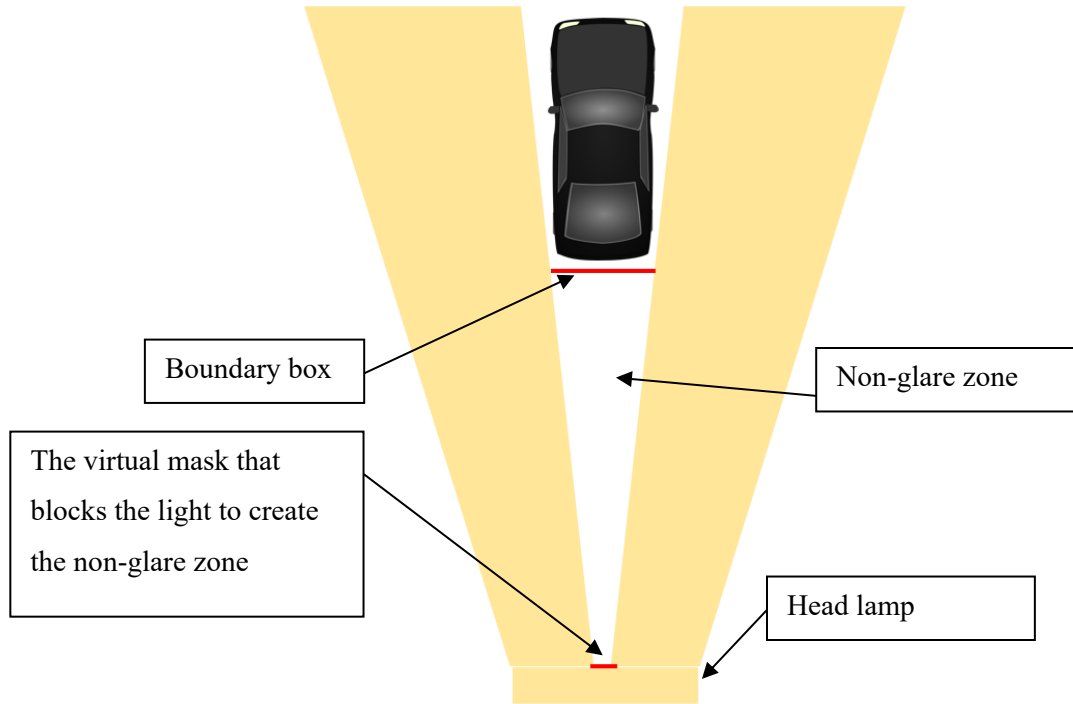


Figure 10. Illustration of pixel masking script, showing that the non-glare zone is created by a virtual mask in front of the lamps.

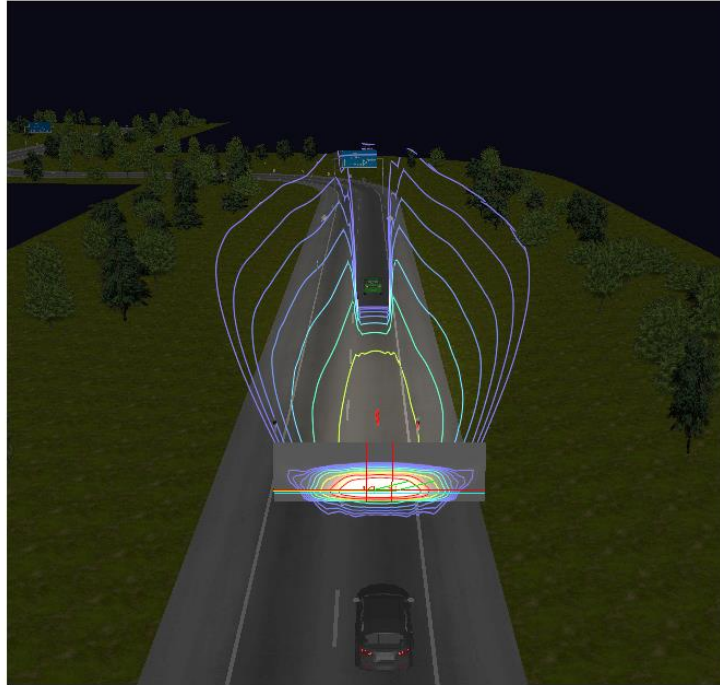


Figure 11. The graphic effect of ADB using pixel masking script in the simulation.

For more accurate control of the width of the boundary box and better illustration of the trade-off relationship between the indirect side rear-view mirror and road illumination, the pixel masking script is chosen to simulate ADB in this research. The beam pattern that is being used in this research is a combined eight-element segmental LED lamp.

2.2. Modification of LucidDrive AFS Plug-in

As discussed in the previous chapter, the input to the ADB system comes from the camera detecting the lamps of other vehicles. In the simulation, since the geometry and the position of the stimulus vehicle are known and assuming the stimulus vehicle is successfully recognized by the system as long as the vehicle is within the designated

region, the built-in AFS simulation module recognizes the stimulus vehicle as a three-dimensional boundary box, shown in Figure 12.



Figure 12. Graphical effect of the three-dimensional boundary box is created for the stimulus vehicle to simulate the vehicle recognition of ADB.

This approach simulates the ideal vehicle recognition result, which is that the entire geometry of the stimulus vehicle can be detected by the system and, thus, the non-glare zone can cover the whole stimulus vehicle. In this case, no glare will be ever created. Since, in reality, only the taillight of the stimulus vehicle is recognized by the system, the boundary should be two-dimensional and surround the rear face of the vehicle, so a modification to the script is needed.

In LucidDrive, the vehicle coordinates system (VCS) refers to the International Organization for Standardization (ISO) 8855 [32][33], where the origin of VCS does not need to be in the center of gravity. In this research, the origin is in the center of the frontal face of the vehicle on the ground, shown in Figure 13. With the input of the length

(L), width (W), and height (H) dimensions of the vehicle's geometry, eight nodes of the three-dimensional boundary box were calculated, which are shown in Figure 14. The modification is off-setting the four nodes of the frontal face of the vehicle with $-L$ along the X-axis, making it overlap with the four nodes on the rear face, which are shown in Figure 15.

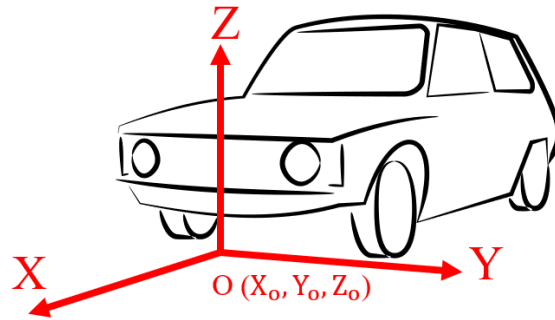


Figure 13. ISO 8855 vehicle coordinate system used in the simulation.

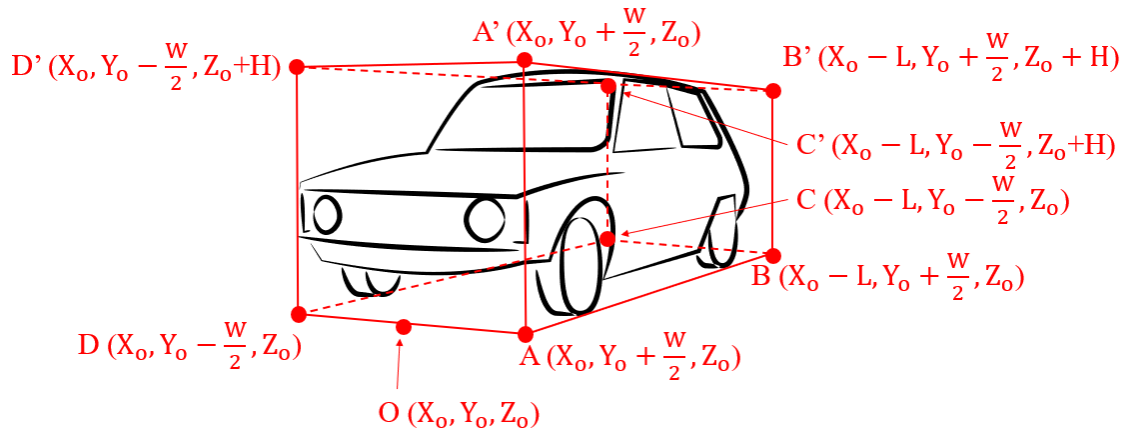


Figure 14. The three-dimensional boundary box of the stimulus vehicle, showing it is generated by the dimension of the vehicle from the origin.

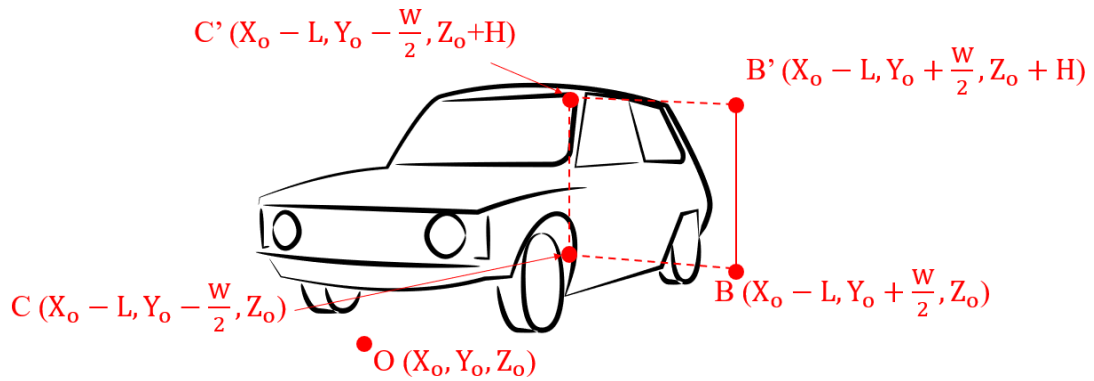
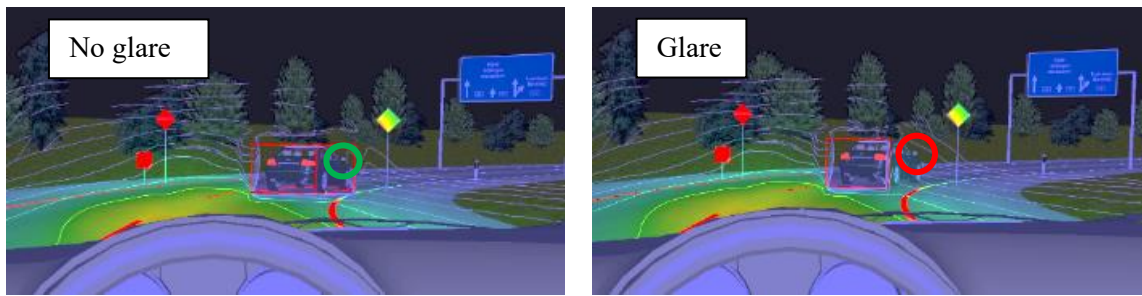


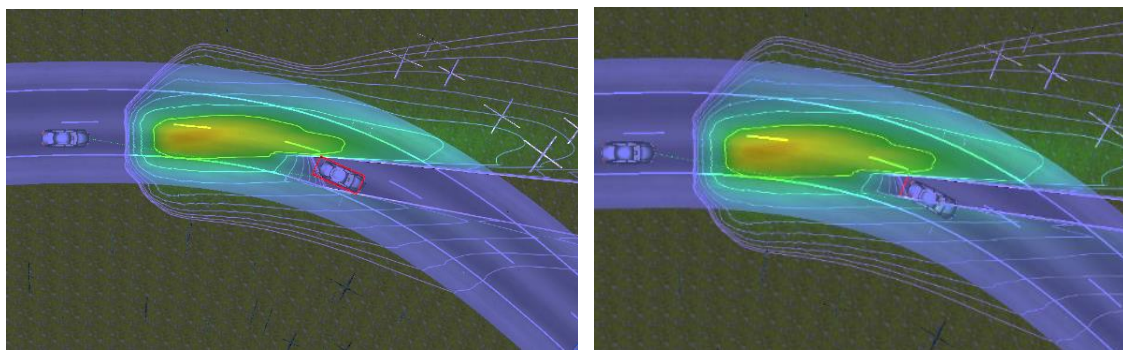
Figure 15. The two-dimensional boundary box of the stimulus vehicle.

Figure 16 provides a graphical comparison between the original and the modified ADB simulation, where the ADB beam pattern, stimulus vehicle, and road geometry along all driving parameters are identical. The non-glare zone width in both simulations is set at 100% of the boundary box. Images (a) and (c) are the original three-dimensional boundary box, and images (b) and (d) show the resultant boundary box after modification, which is a two-dimensional plane parallel to the rear of the vehicle that can better simulate real driving scenarios. From the comparison of the driver views, it can be seen that, with the modification, the side rear-view mirror (circled in green) that was originally included in the non-glare zone (Figure 16(a)) is now exposed in the glare zone (Figure 16 (b)), highlighted with the red circle. It can also be seen from the top view, although the non-glare zone setting is the same as 100%; with the modification of the boundary box, the resultant non-glare zone is significantly narrower. As a result, the frontal part of the stimulus vehicle was exposed (Figure 16 (d)), compared to Figure 16 (c), where the entire vehicle is in the non-glare zone. This indicates the glare issue was successfully reproduced in the simulation with the modification.



(a) Original AFS driver view

(b) Modified AFS driver view



(c) Original AFS top view

(d) Modified AFS top view

Figure 16. A graphical comparison in the simulator between the original and the modified ADB simulation, where the non-glare zone is set at 100% and all parameters are identical. The red lines around the stimulus vehicle represent the boundary box. (a) and (c) are the original ADB simulation where the three-dimensional boundary box is recognized, and, thus, the entire vehicle geometry is covered by the non-glare zone. The modification in (b) and (d) simulates a more realistic ADB, in which only the tail-light is recognized; thus, in top view (d), it is just a line at the rear of the stimulus vehicle. The non-glare zone is highlighted with yellow dashed lines showing that, with the modification, the side rear-view mirror will be excluded from the boundary box during the cornering maneuver. The comparison shows that the simulator’s modified AFS plug-in can reproduce the glare issue.

After the side rearview mirror glare issue was successfully reproduced in the night drive simulator, the next step is to reproduce the tuning of the non-glare zone width,

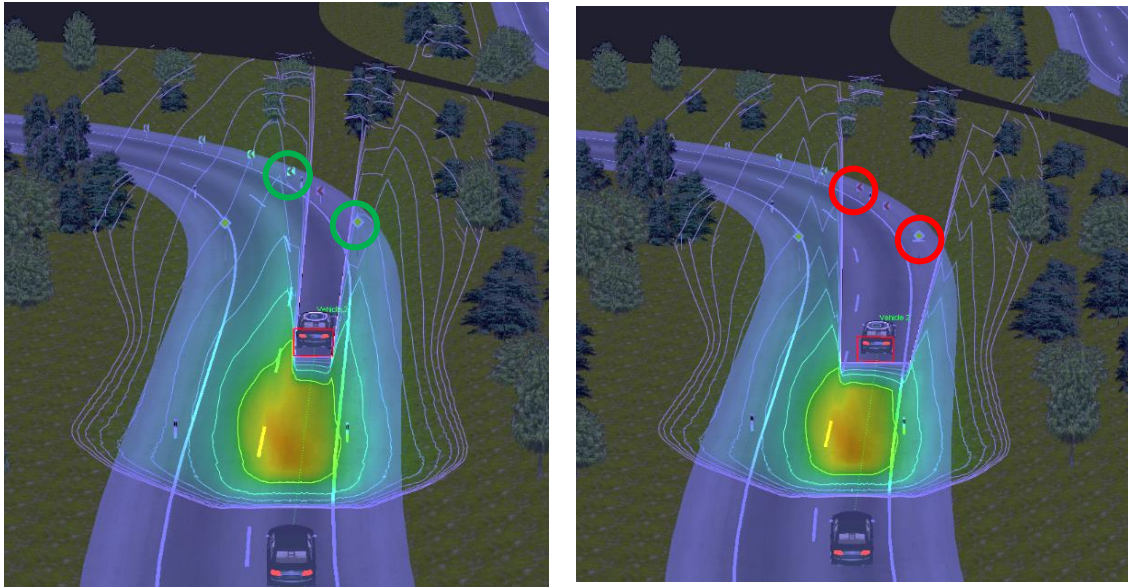
showing that the glare can be eliminated when widening the non-glare zone. Figure 17 and Figure 18 demonstrate how altering the non-glare zone width would affect glare and road illumination by comparing an ADB with 100% non-glare zone to one with 150% in the same driving scenario. The width of the non-glare zone is measured as the percentage with respect to the width of the boundary box. A 100% non-glare zone width means it is the same width as the boundary box, which is the narrowest; a 150% non-glare zone width means it widens (equally on both the left and right) to 150% of the boundary box width. In Figure 17(a), the rear-view mirror, highlighted in the red circle, is not covered by the non-glare zone, and, thus, glare is created. By increasing the non-glare zone width to 150% of the boundary box, shown in Figure 17(b), glare is eliminated in the rear-view mirror, highlighted in a green circle, indicating a good experience. Meanwhile, in terms of road illumination, with a 100% non-glare zone width, the two circled street signs in Figure 18(a) are illuminated, while Figure 18(b) shows that they are not in a widened non-glare zone, indicating worse road illumination. This shows that, although widening the non-glare zone could solve the side rear-view's mirror indirect glare issues, the narrower non-glare zone provides better visibility to the driver, who can observe the surrounding environment and road conditions more effectively. For example, if a deer is standing by the roadside, the ADB system with a narrower non-glare zone will illuminate the deer sooner, giving the driver more reaction time, thus enhancing driving safety. This comparison indicates the importance of defining the best non-glare zone width that balances glare mitigation and driver visibility..



(a) 100% non-glare zone width (glare).

(b) 150% non-glare zone width (no glare).

Figure 17. Effect on glare when altering non-glare zone width, showing that widening the non-glare zone could effectively eliminate glare.



(a) 100% non-glare zone width (better road illumination).

(b) 150% non-glare zone width (worse road illumination).

Figure 18. Effect on road illumination when altering non-glare zone width, showing that widened non-glare zone sacrifice road illumination. For example, the traffic signs circled on (a) are well illuminated, however, when the non-glare zone increases on (b), the signs are included in the non-glare zone and, thus, are not illuminated. This indicates the driver will have better and wider visibility with the narrower non-glare zone, which enhances driving safety.

2.3. *Driving Scenario Design*

To further investigate this trade-off effect between glare and road illumination, four S-curve driving scenarios are designed, which are shown in Figure 19. The designs are based on the road shown in Figure 1. All four S-curves are designed with a track transition curve[34] with the minimum curvature of 25 m, 50 m, 75 m, and 100 m, shown in Figure 21. Track transition curves are commonly used in modern road design, providing a gradual change in the curvature of the driving path to avoid a sudden change

in lateral acceleration [35]. Figure 19 and Figure 20 show the curvature of the driving path and the lateral acceleration of the vehicle driving on an S-curve designed with a track transition curve with a minimum curvature at 25 m (Figure 21(a)), where the vehicle enters the corner at around 22 s and leave the corner at around 43 s. There is some noise in the data at around 33 s when the vehicle is at the inflection point of the S-curve. Before 22 s and after 43 s, the vehicle travels on a straight road, and any slight steering input results in a large curvature, reflected as those vertical lines on the graph.

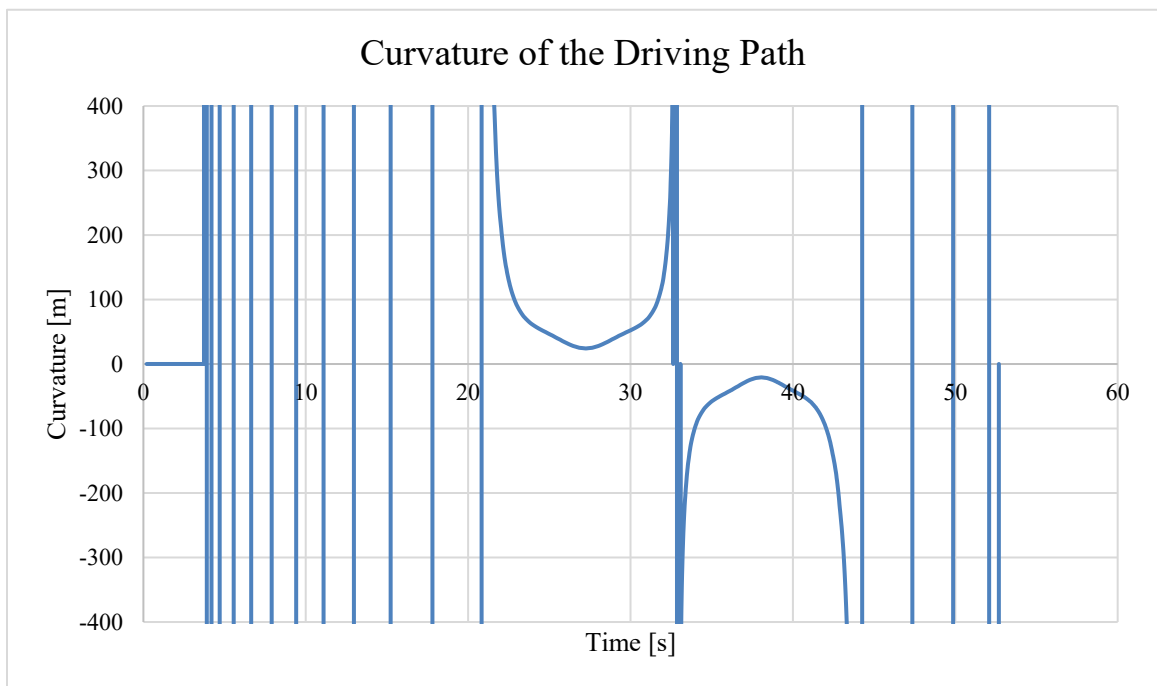


Figure 19. Curvature of the driving path of the vehicle driving on a track transition curve with a minimum curvature of 25 m, showing that it gradually changes during the corner.

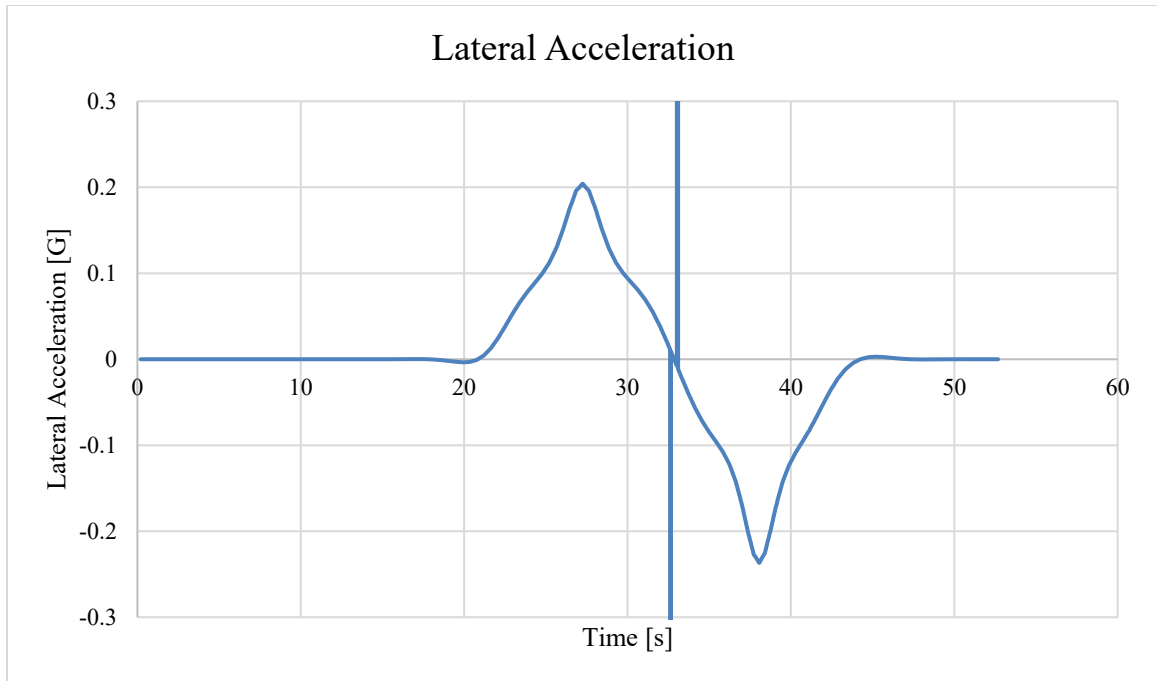


Figure 20. Lateral acceleration of the vehicle driving on a track transition curve with a minimum curvature of 25 m, showing that it gradually changes during the corner.

Those curvature designs are based on the speed of the ADB vehicle, calculated by the formula (1) of curve design guidelines provided by the *A policy on geometric design of highways and streets* from the American Association of State Highway and Transportation Officials (AASHTO) [35], also known as the Green Book.

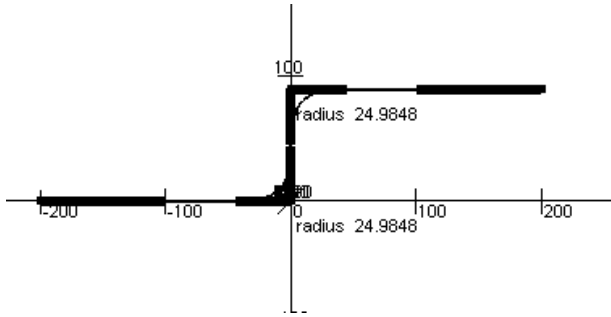
$$R_{min} = \frac{V_d^2}{127(e + f_{max})} \quad (1)$$

Where:

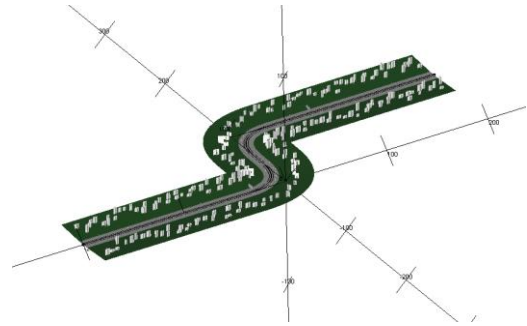
- R_{min} is the minimum curvature;
- V_d is the advisory speed;

- e is the superelevation, which is 0 in this case, as suggested by NHTSA for ADB testing in NPRM[14]; and
- f_{max} is the comfortable side friction factor referenced from the Green Book [35].

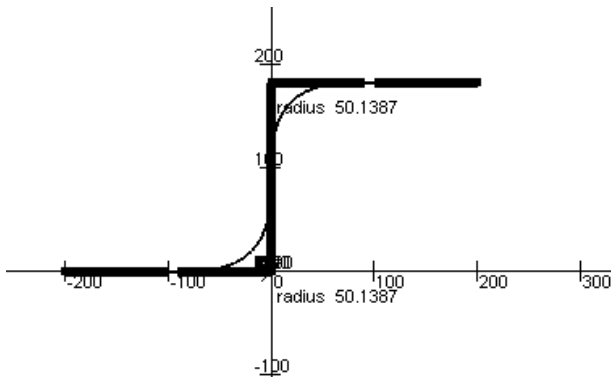
The 100 m curvature corresponds to a genetic ADB activation speed of 45 km/h, which is also the minimum curvature that NHTSA proposed for ADB testing. The ADB function of the most current production vehicle will automatically be activated when the vehicle speed exceeds the activation speed. The deactivation speed of ADB, however, is usually lower than the activation speed. A study from NHTSA shows that ADB deactivation speed can be as low as 25 km/h [36]. Thus, if a vehicle travelling with ADB enabled encounters a curve with a curvature as low as 25 m, the ADB will not be deactivated. The 50 m and 75 m curves are included to study the influence of curvature on optimized non-glare zone width.



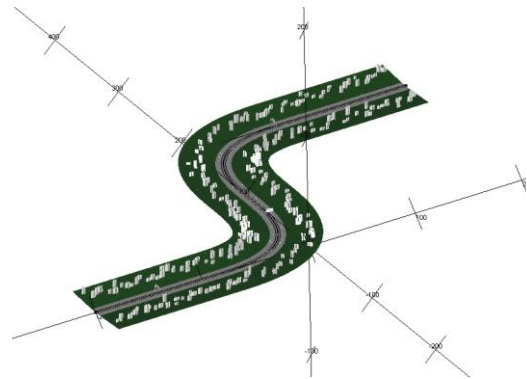
(a) Planar graph of S-Curve with minimum curvature at 25 m



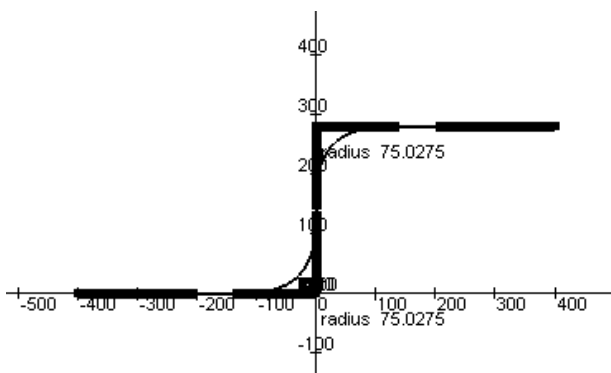
(b) Rendering of S-Curve with minimum curvature at 25 m



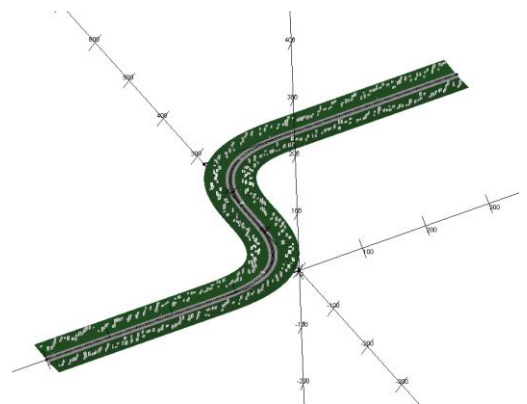
(c) Planar graph of S-Curve with minimum curvature at 50 m



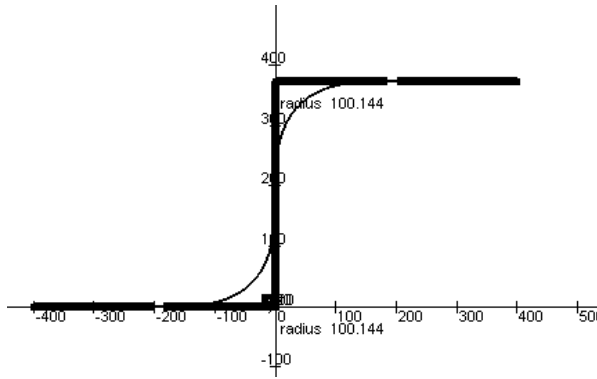
(d) Rendering of S-Curve with minimum curvature at 50 m



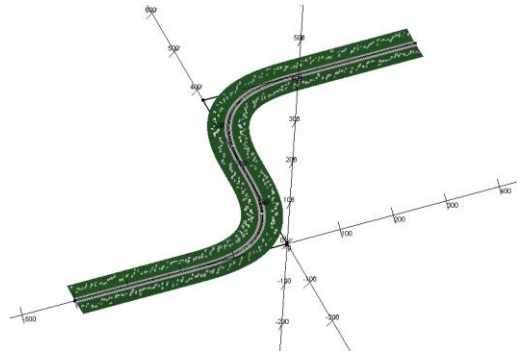
(e) Planar graph of S-Curve with minimum curvature at 75 m



(f) Rendering of S-Curve with minimum curvature at 75 m



(g) Planar graph of S-Curve with minimum curvature at 100 m



(h) Rendering of S-Curve with minimum curvature at 100 m

Figure 21. Driving scenarios prepared for the virtual night drive data collection. The curve varies from 25 m to 100 m, with the 25 m curvature corresponding to a vehicle travelling at minimum ADB deactivation speed, below which the ADB will automatically be deactivated and switch to low beam. The 100 m curvature corresponds to the minimum curvature that NHTSA proposed for ADB testing in NPRM [14]

The following distance between the two vehicles is calculated by the three-second rule, suggested by the National Safety Council of the United States[37], assuming there are safe driving conditions. The complete set of parameters of the four driving scenarios for this research are shown in Table 1.

Table 1. Parameters of the driving scenario

Curvature [m]	Side Friction Coefficient [-]	Speed [km/h]	Rounded Speed [km/h]	Following Distance [m]
25	0.18	23.9	25	20
50	0.17	32.8	30	25
75	0.17	40.2	40	30
100	0.16	45.1	45	40

2.4. Virtual Stimulus Vehicle and Light Sensor

As mentioned earlier, Out of the box, LucidDrive is not designed for and not capable of performing data collection. A new virtual light sensor was implemented in the software for this research. The method involves calculating the relative position of the sensor point to the ADB head beam then extracting data from the beam pattern file. Compared to real-time raytracing, this method is less time-consuming and computationally cheaper, while still accurate.

The selection of stimulus vehicle and sensor position in this research is based on the SAE J3069 [14] ADB test fixture. From the vehicle geometry pool in LucidDrive, a Mercedes-Benz E W211 vehicle geometry is chosen as the stimulus vehicle, considering that its dimensions are similar to the test fixture. The light sensor is mounted 0.9 m above

the ground, 0.9 m away from the center along the y-axis, and 3.5 m away from the rear of the vehicle along the x-axis, representing the position of the driver-side rearview mirror, illustrated in Figure 22 and Figure 23.

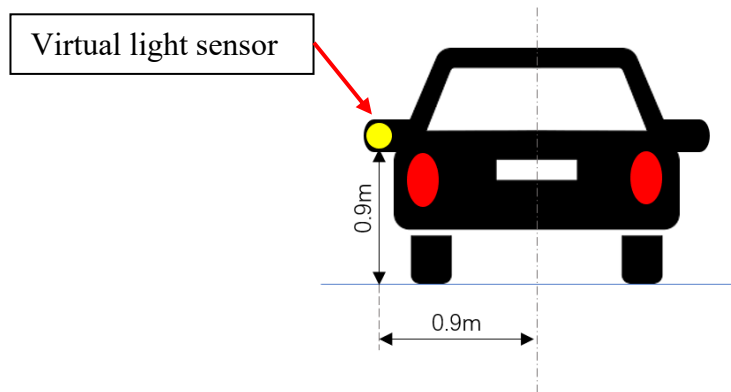


Figure 22. The position of the virtual light sensor, which corresponds to the ADB test fixture from SAE J3069 [14].

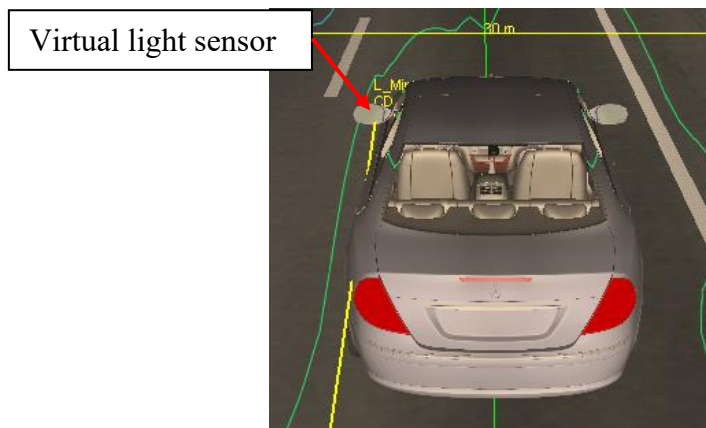


Figure 23. Rear view of the stimulus vehicle and the position of the virtual lux meter in the simulation.

In summary, this chapter discussed the preparation and set-up of the simulation tool for this research, explaining how the LucidDrive is customized to realistically simulate an ADB vehicle cornering in order to reproduce the side rearview mirror issue,

as well as the demonstrating the trade-off effect between road illumination and glare. This chapter also discussed the design of the four virtual night drive scenarios that will be used to study the non-glare zone width in different curvatures. The next chapter will discuss the virtual night drive test and data collection, as well as post-processing, which uses a fuzzy logic controller to mimic a human driver to find the best non-glare zone width.

CHAPTER 3

DATA COLLECTION AND POST-PROCESSING

After the customization of the night drive simulator – changing the boundary box from the default three-dimensional to two-dimensional, as discussed in the previous chapter – LucidDrive is now capable of simulating ADB more realistically. Also, the test road design is finished as well as the implication of the virtual sensor. This chapter discusses the execution of the test. Since this research aims to use a fuzzy logic controller to mimic human subjective lighting evaluation to find the best non-glare zone, the first step is to acquire data as input to the controller.

3.1. Data Acquired from LucidDrive

In each driving scenario, the vehicle starts from the left end of the road, then navigates a left turn followed by a right turn, and finishes at a straight road. Because the overall length of the road also increases when the curvature increases, the simulation time varies from around one to two minutes. The lux reading of each simulation is logged, and a lux-time graph is plotted. Figure 24 shows the data collected for the narrowest non-glare zone in the first driving scenario in which the minimum curvature is 25 m.

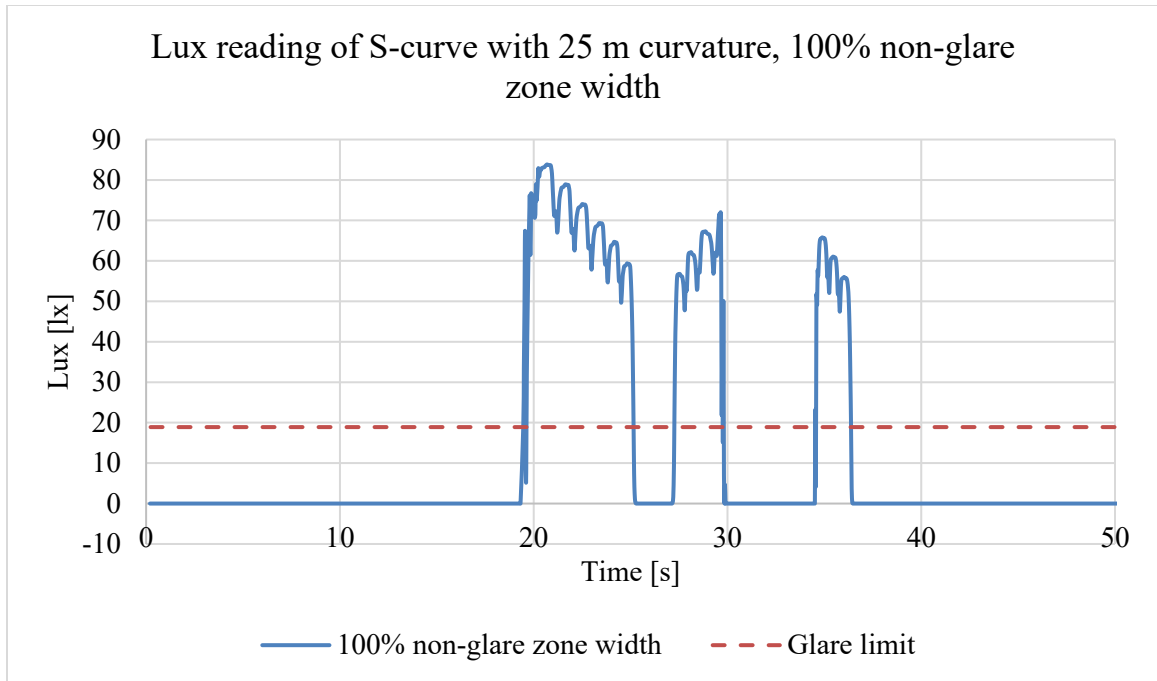
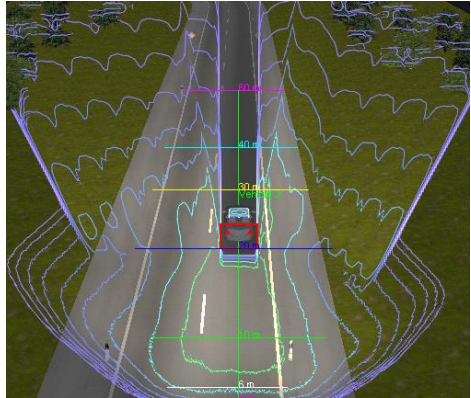


Figure 24. Lux reading of S-curve with 25 m curvature simulation at 100% non-glare zone width. The dashed line is 18.9 lux, above which is considered to be glare, according to both NHTSA [14] and SAE [15].

At the beginning of the simulation, between 0 and 20 seconds, the vehicle travels on a straight road (Figure 25 (a)), where zero glare is created. When the stimulus vehicle enters the corner at around 20 seconds (Figure 25 (b)), the side rear-view mirror shifts away from the non-glare zone, and, thus, glare is created, which is reflected as the first spike on the lux-time graph. As the vehicle continues the left turn (Figure 25 (c)), there is a brief time when the stimulus vehicle exits the high beam zone of the test vehicle during which the lux reading drops to zero for a few seconds; then, glare is again observed when the test vehicle enters the corner, reflected in the graph as the second spike. When the vehicle enters the right turn, no glare should be created from the driver-side rear-view mirror, since the light is blocked by the vehicle body (Figure 25 (d)). The third spike in

the lux-time graph is due to the limitation of the simulator – its lack of ray-tracing technology – causing the light to reach the sensor by penetrating through the vehicle geometry. This is considered an error and will be neglected during data processing.



(a) At the beginning of the simulation, the vehicle travels on a straight road, and no glare is created.



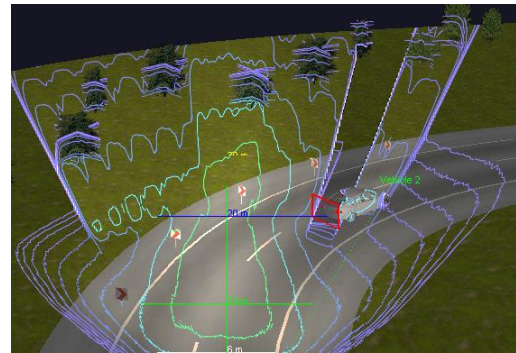
(b) When the vehicle enters the corner, glare is created, corresponding to the first peak in Figure 24.

24.



(c) When the stimulus vehicle exit the high beam area, there is a short time when glare drops to zero, corresponding to the area between two peaks in

Figure 24.



(d) Light penetrates through the vehicle body due to the limitation of the simulator, which is shown as the third peak in Figure 24 and is neglected as

an error.

Figure 25. S-curve with 25 m curvature simulation at 100% non-glare zone width.

In accordance with the NHTSA ADB testing proposal [14] and the SAE standard ADB testing procedure [15] and for the same direction driving scenario at a distance shorter than 60 m, lux readings above 18.9 lx are considered to be glare, which is the dashed line in Figure 24. In this project, the total time during a simulation when the lux reading is above 18.9 lx is considered as the glare rating for this driving scenario and will be used as an input in the fuzzy logic controller to find the best non-glare zone width.

As shown in Figure 26, with increases in non-glare zone width, not only does the total glare time reduce, (shown in Figure 27), but also the lux peak reduces. It is noted that, when the non-glare zone increases from 140% to 180%, the second lux peak (around 27 s to 30 s) is eliminated. Finally, when the non-glare zone width is increased to 265% of the boundary box width, all lux readings are below the 18.9 lx limit, so glare can be considered to be eliminated. 265% is the upper limit of the non-glare zone width for a 25 m curvature cornering driving scenario when road illumination is the worst.

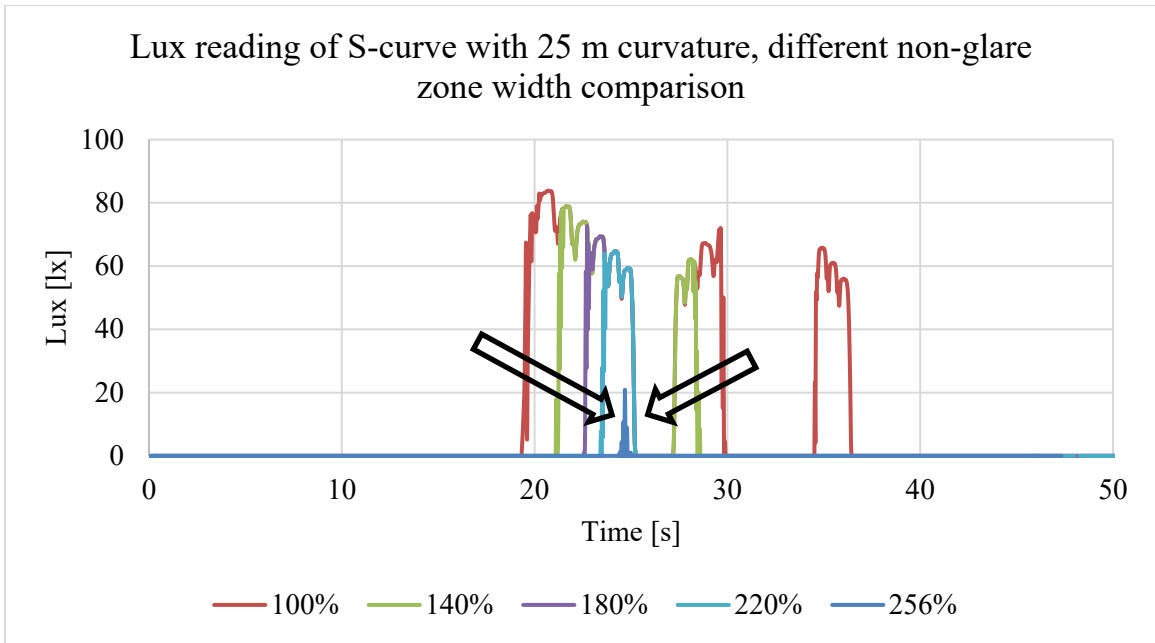


Figure 26. Lux reading of S-curve with 25 m curvature simulation in different non-glare zone width, showing the trend of glare reduction with increasing non-glare zone width.

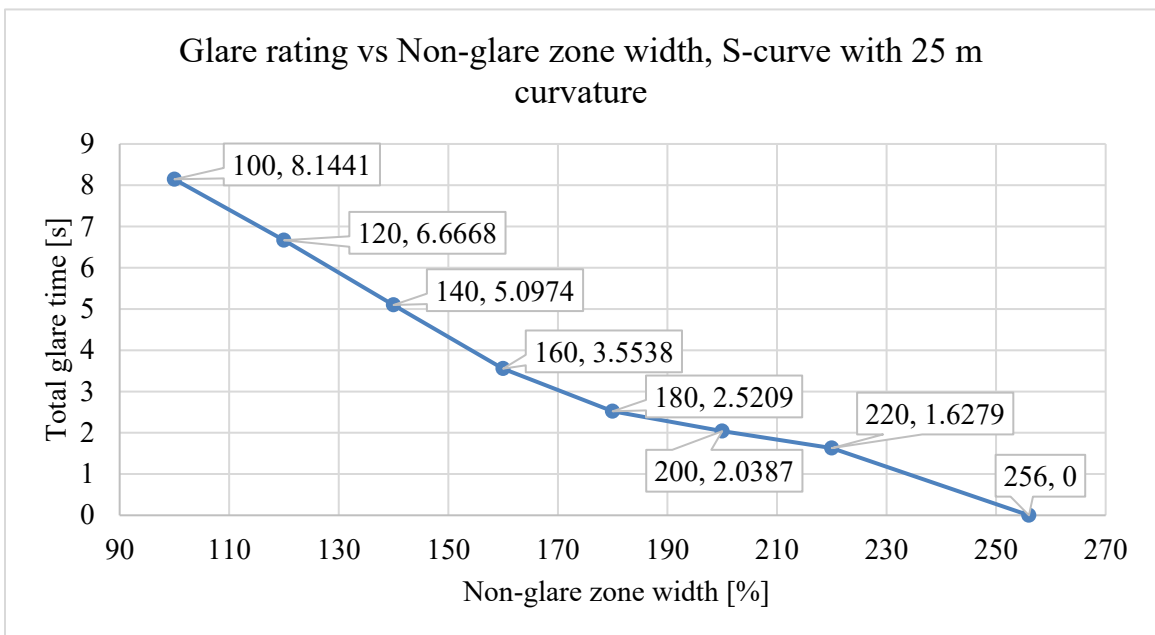


Figure 27. Total glare time vs. non-glare zone width for S-curve with 25 m curvature, showing that the total glare time reduces with increasing non-glare zone width. All glare is eliminated if the non-glare zone widens to 256% of the boundary box's width.

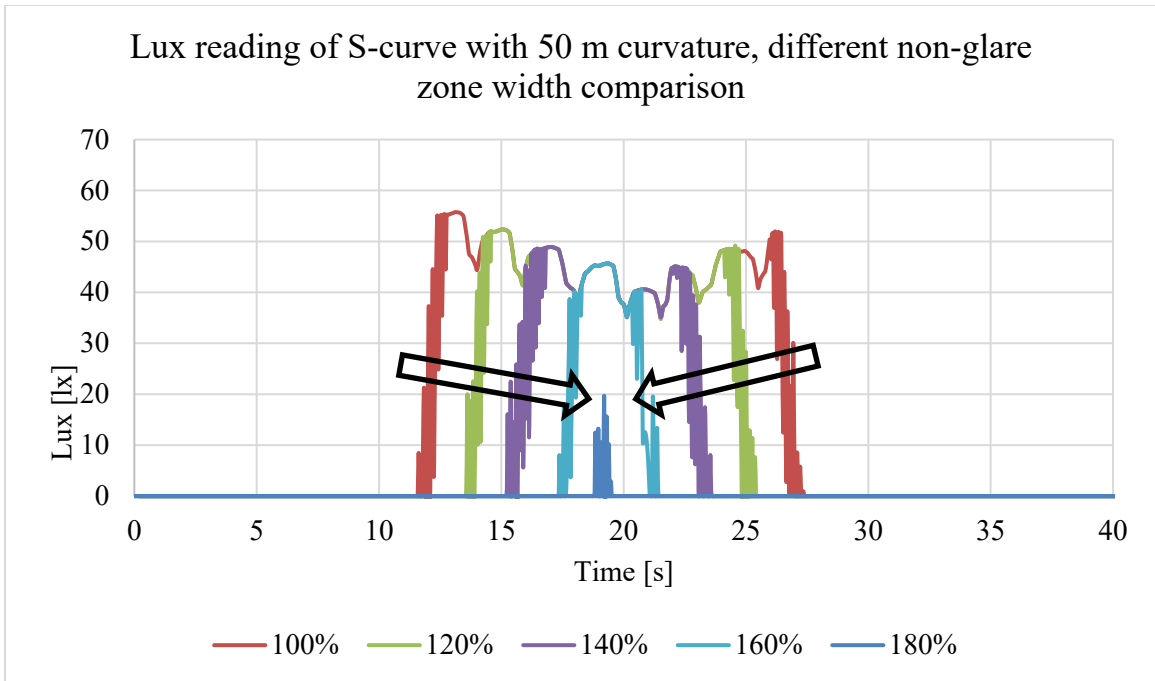


Figure 28. Lux reading of S-curve with 50 m curvature simulation in different non-glare zone width.

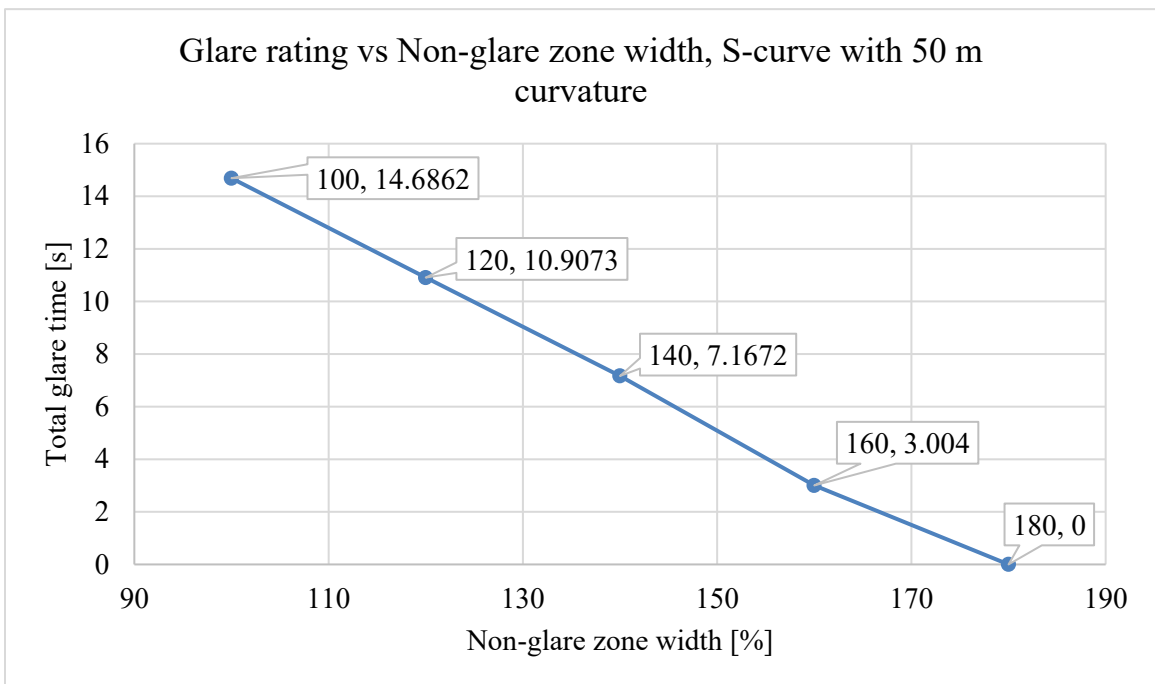


Figure 29. S-curve with 50 m curvature, total glare time vs. non-glare zone width.

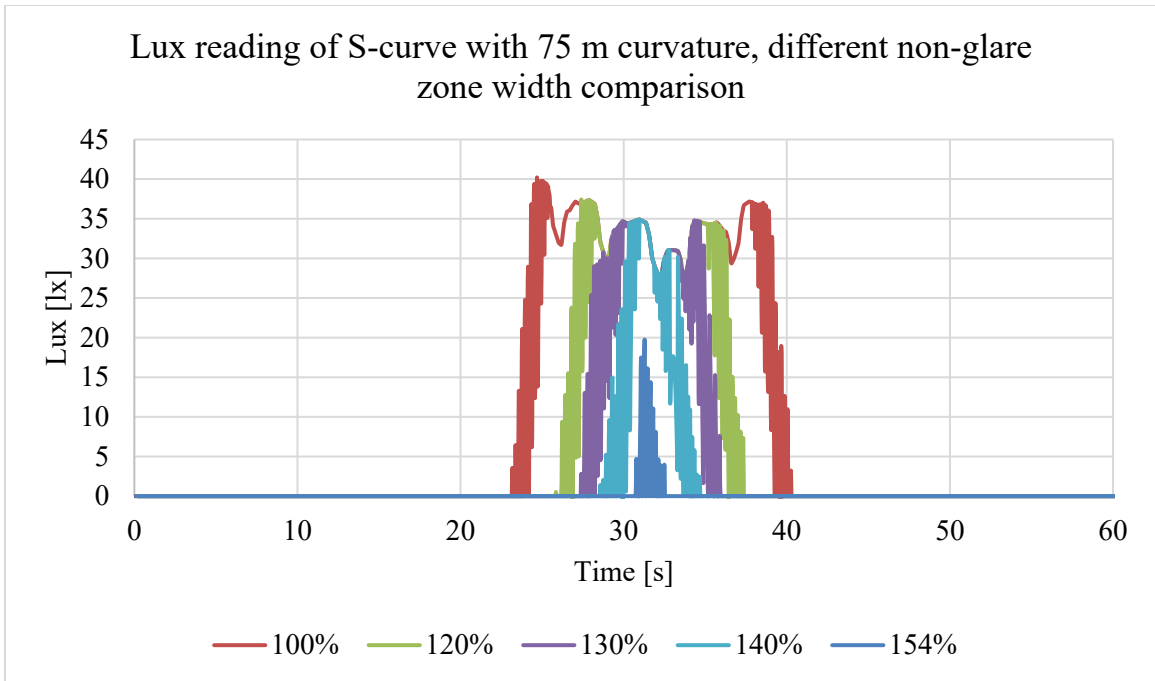


Figure 30. Lux reading of S-curve with 75 m curvature simulation in different non-glare zone width.

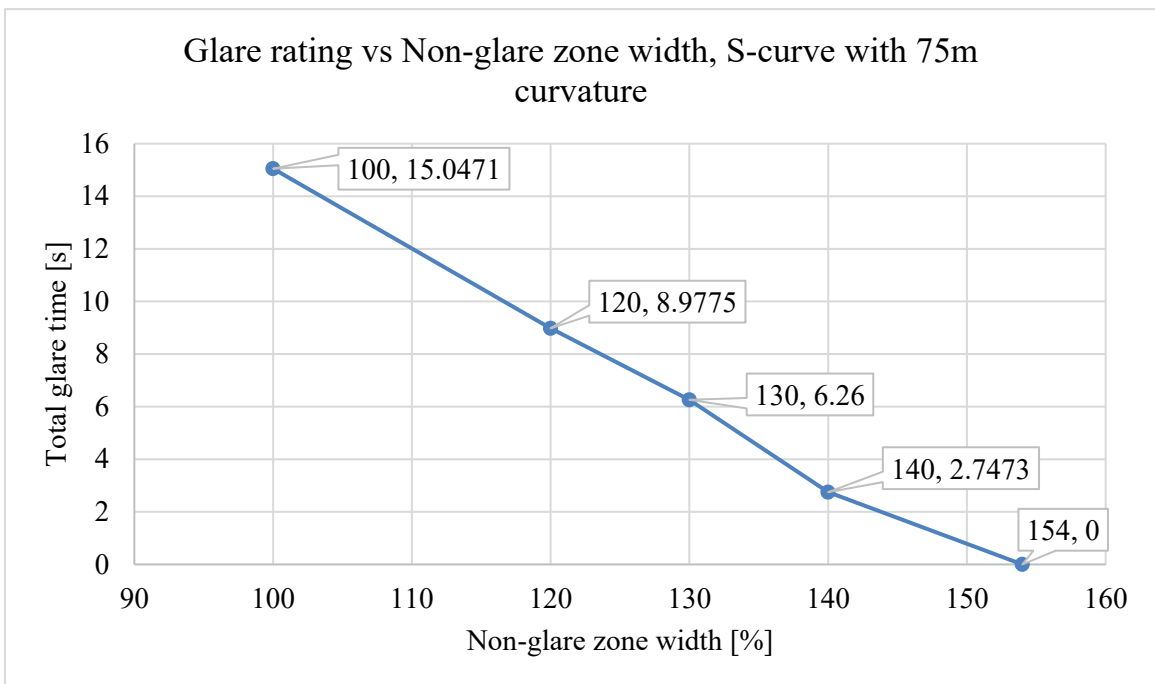


Figure 31. S-curve with 75 m curvature, total glare time vs. non-glare zone width.

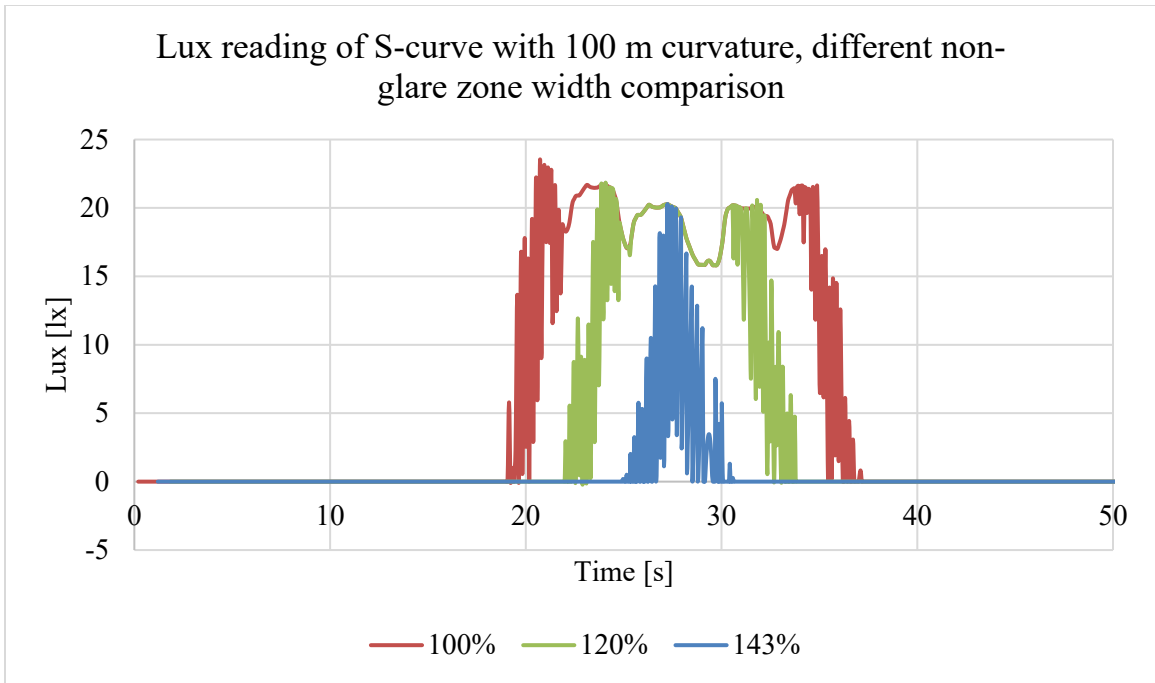


Figure 32. Lux reading of S-curve with 100 m curvature simulation in different non-glare zone width.

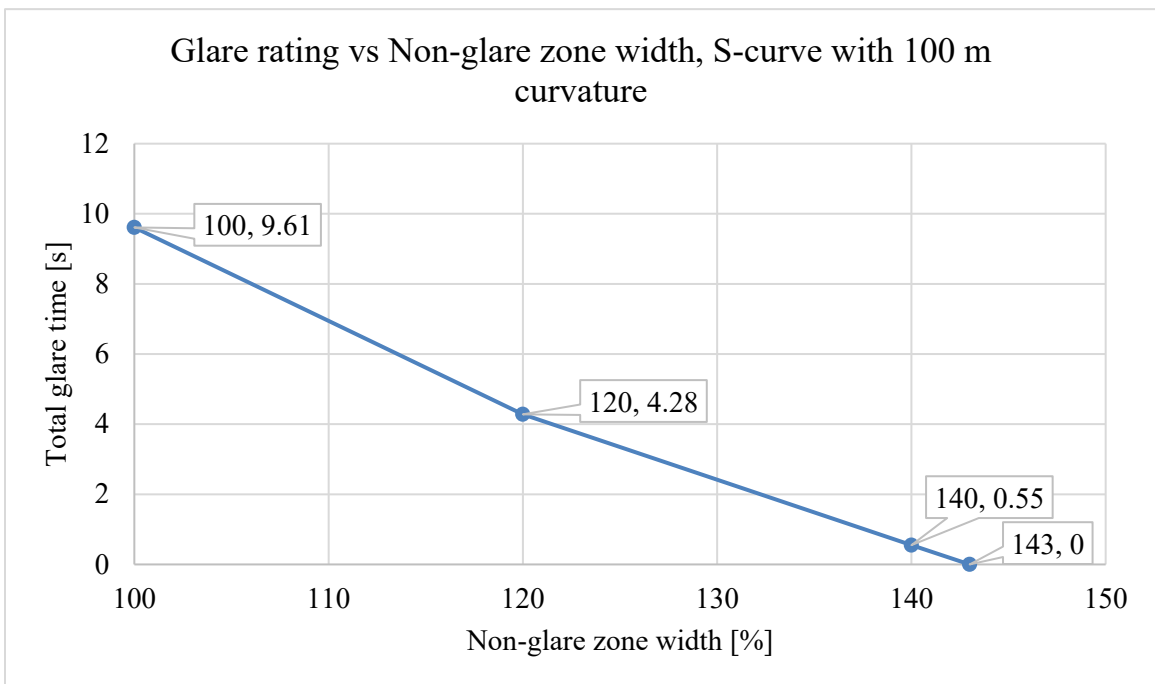


Figure 33. S-curve with 100 m curvature, total glare time vs. non-glare zone width.

3.2. Fuzzy Logic Controller

Fuzzy logic was first introduced in 1965 by Zadeh [38]. It is designed to handle the concept of partial truth, which is close to human semantic statements in which the truth is mostly partial and imprecise. Unlike classical logic that operates at either true or false, fuzzy logic operates with continuous values between the two extremes: completely true and completely false. Similar to how the color grey is found between black and white, fuzzy logic can present imprecise linguistic expressions such as “slightly”, “quite”, or “very”. Fuzzy logic has been employed in many applications such as temperature control of air conditioners and suction power control in vacuum cleaners, amongst others.

The data acquired from the simulator is then processed in MATLAB with a Fuzzy Logic Toolbox [39]. This project aims to provide automotive OEMs with an efficient and less time-consuming methodology for studying ADB non-glare zone width. Considering the use of a human test driver to evaluate the performance of a vehicle headlamp, both glare and road illumination cannot be precisely stated between just two opinions: good or bad. Choosing the best value of the non-glare zone width that balances the glare and road illumination is not a dichotomous situation. A fuzzy logic controller is a good candidate to mimic a human test driver in providing feedback and finding the best value in this application, as it not only takes continuous input but also does not require a precise mathematical model nor a large volume of data. Instead, it is simply based on logic, making it less time-consuming and less computationally expensive.

As shown in Figure 34, the two inputs to the controller are the glare rating and the road illumination rating. The glare rating is represented by the overall time that the lux

reading is above the glare limit in a simulation, as discussed in the previous section. The road illumination rating can be represented by the non-glare zone width; this is because the road illumination is at its best when the non-glare zone is at its narrowest, and at its worst when the non-glare zone is at its widest. Thus, they can be seen as inversely proportional. The wider the non-glare zone, the less area that is covered by the high beam area that benefits from the dynamic beam pattern of the ADB. The output of the controller is the change in non-glare zone width.

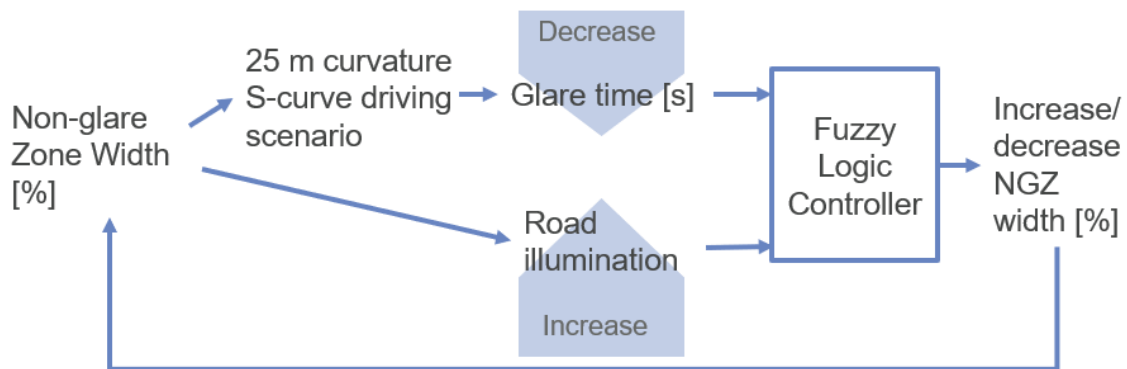


Figure 34. Schematic show fuzzy logic controller block diagram.

Both inputs use two membership functions to represent good and bad performance. The “good” membership functions represent a low glare time and a narrow non-glare zone that results in good road illumination, while the “bad” membership functions represent the opposite. The output uses three membership functions to indicate that the non-glare zone width should be increased, decreased, or if it is just good. The fuzzy logic controller is based on three rules:

- if both road illumination and glare are good, then the non-glare zone width is good;

- if the road illumination is poor while the glare is good, the non-glare zone width should be increased; and
- if the road illumination is good, while the glare is poor, then the non-glare zone width can be reduced.

Two trials are presented in this research using different basic membership functions to find the best non-glare zone width. The first trial uses linear triangular membership functions, and the second trial uses Gaussian membership functions, as shown in Figure 35.

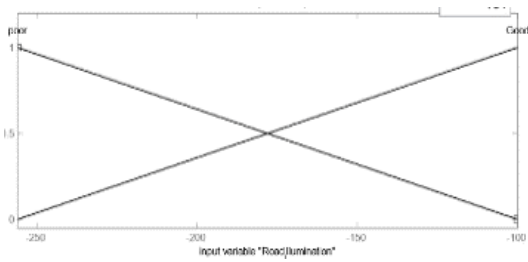
The parameters of the unscaled membership functions are shown in Table 2. The range of the inputs is considered as spanning from the worst case to the best case. For input on the road illumination, the best case is when the non-glare zone is at its minimum, which is 100% of the width of the boundary box; the worst case is when it is the widest, with all glare eliminated in all driving scenarios, which is 256% of the boundary box width. For the glare rating, the worst case is the overall glare duration at the 100% non-glare zone width at each driving scenario, while the best case is 0 s of glare, indicating that it is glare-free. These details are shown in Table 3. This research aims to demonstrate the methodology of using fuzzy logic to mimic human feedback. The parameters can be seen as an initial guess and would require a physical test for fine-tuning, which is considered to be future work and not included in this research. The parameters are also expected to vary from case to case with different ADB systems and different beam patterns.

Table 2. Parameters of the unscaled membership functions, range 0-1

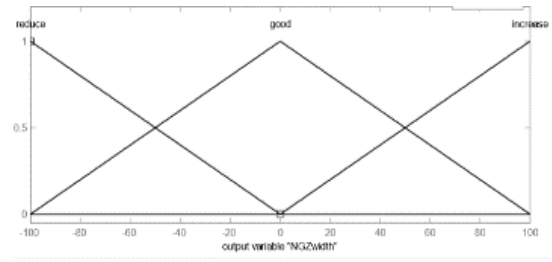
	Input		Output		
Function names	good	bad	increase	good	decrease
Trimf parameters	[0 1 2]	[-1 0 1]	[0.5 1 1.5]	[0 0.5 1]	[-0.5 0 0.5]
Gaussmf parameters	[0.4247 1]	[0.4247 0]	[0.2123 1]	[0.2123 0.5]	[0.2123 0]

Table 3. Variable range of the membership functions

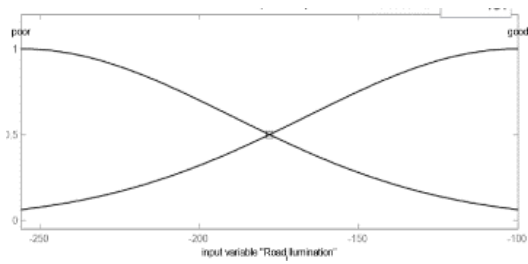
Driving Scenario	Glare	Road Illumination	Change in Non-Glare Zone Width
S-curve with 25 m curvature	0 ~ 8.144	100 ~ 256	-100 ~ 100
S-curve with 50 m curvature	0 ~ 14.686		
S-curve with 75 m curvature	0 ~ 15.047		
S-curve with 100 m curvature	0 ~ 9.61		



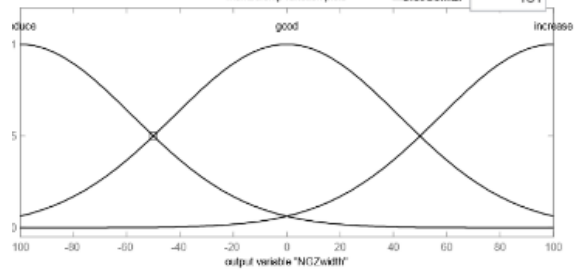
Road illumination input triangular membership function in Trial 1



Change in non-glare zone width output triangular membership function in Trial 1



Road illumination input Gaussian membership function in Trial 2



Change in non-glare zone width output Gaussian membership function in Trial 1

Figure 35. Membership function of fuzzy logic controller.

The iterations of the optimization in four driving scenarios are shown in Table 4 and Table 5, where the last columns are the outputs from the fuzzy logic controller, which were added to the non-glare zone width for the next iterations. The best non-glare zone width is recorded when the output change in non-glare zone width is less than 0.5%. The two demonstrated trials show different iteration. Trial 1 took four-to-five iterations to converge at the optimal glare-free zone, while Trial 2 took six-to-seven iterations. This shows that different types of membership functions are able to converge in an optimal non-glare zone. A correlation study of physical tests would help to select the membership function type and its parameters in future work.

Table 4. Trial 1 iteration of four driving scenarios, using the fuzzy logic controller with linear membership function

Driving Scenario	Iteration	Non-Glare Zone Width [%]	Glare Rating [s]	Output [%]
S-curve with 25 m curvature	1	256	0	-105
	2	151	4.2	-2.3
	3	149	4.4	-0.53
	4	148	4.5	-0.06
S-curve with 50 m curvature	1	180	0	-20
	2	160	3	-7.93
	3	152.3	4.6	-0.885
	4	151	4.8	-0.008
S-curve with 75 m curvature	1	154	0	-9.34
	2	144.7	1.7	-5.2
	3	138.4	3.1	-1.17

	4	137.2	3.6	-0.23
	5	137	3.6	0.274
S-curve with 100 m curvature	1	143	0	-3.87
	2	139.1	1.1	-2.82
	3	136.3	1.2	-2
	4	134.3	1.8	-0.785
	5	133.5	1.9	-0.5

Table 5. Trial 2 iteration of four driving scenarios, using the fuzzy logic controller with Gauss membership function

Driving Scenario	Iteration	Non-Glare Zone Width [%]	Glare Rating [s]	Output [%]
S-curve with 25	1	256	0	-55.7
	2	200.3	2	-25.1

m curvature	3	175.2	2.6	-7.09
	4	168.11	3.1	-2.36
	5	165.75	3.2	-1.86
	6	163.89	3.4	0.367
S-curve with 50 m curvature	1	180	0	-13.9
	2	166.1	2	-7.6
	3	158.5	2.6	-4.86
	4	153.64	4.2	-1.64
	5	152	4.3	-1.13
	6	150.87	4.5	-0.308
S-curve with 75 m curvature	1	154	0	-4.74
	2	149.26	1	-3.54
	3	145.72	1.6	-2.75

	4	142.97	2.2	-2
	5	140.97	2.6	-1.44
	6	139.53	2.8	-1.15
	7	138.38	3.1	-0.67
S-curve with 100 m curvature	1	143	0	-2.62
	2	140.38	0.5	-2.16
	3	138.22	0.9	-1.71
	4	136.51	1.22	-1.3
	5	135.21	1.4	-1
	6	134.21	1.6	-0.7
	7	133.51	1.75	-0.45

3.3. *Result*

Table 6 and Figure 36 show the result of the best non-glare zone width in different driving scenarios. The x-axis is the minimum curvature of the driving scenario and the y-axis is the best non-glare zone width defined by the fuzzy logic controller. The top dashed line is the non-glare zone width when all glare is eliminated, which is in the extreme case of the best glare rating and the worst road illumination. The x-axis also represents the narrowest non-glare zone width, which is just as wide as the vehicle boundary box, when the road illumination rating is the best and the glare rating is the worst. The best value of the non-glare zone width should lie between these two lines, balancing the glare/road illumination trade-off. The two solid lines are the first and second trials of the fuzzy logic controllers using different membership functions. Those can be considered as two balances of the road illumination and glare trade-off. Those two trials have very similar results, except in the S-curve with 25 m minimum curvature, where the second trial prefers lower glare and the first one prefers better road illumination.

Such results could be used as an ADB non-glare zone width design guideline for automotive OEMs. For example, if an OEM would like to consider the performance of this ADB system at corner curvature as low as 50m, the non-glare zone width should be set at 151% of the boundary box according to the result, balancing the glare and road illumination. Note that the minimum curvature proposed by NHTSA for ADB testing in NPRM is 100m. If the proposed ADB testing procedure is executed, then the minimum non-glare zone width of this ADB should be set to 143% of the boundary box to meet the legal requirement.

Table 6. Best non-glare zone width vs. minimum curvature of the S-curve in all four driving scenario simulations

Driving Scenario	Minimum Curvature [m]	Optimal Non-Glare Zone Width [%] Trial 1	Optimal Non-Glare Zone Width [%] Trial 2	Glare-Free Non-Glare Zone Width[%]
1	25	148	164	256
2	50	151	150	180
3	75	137	138	154
4	100	133	133	143

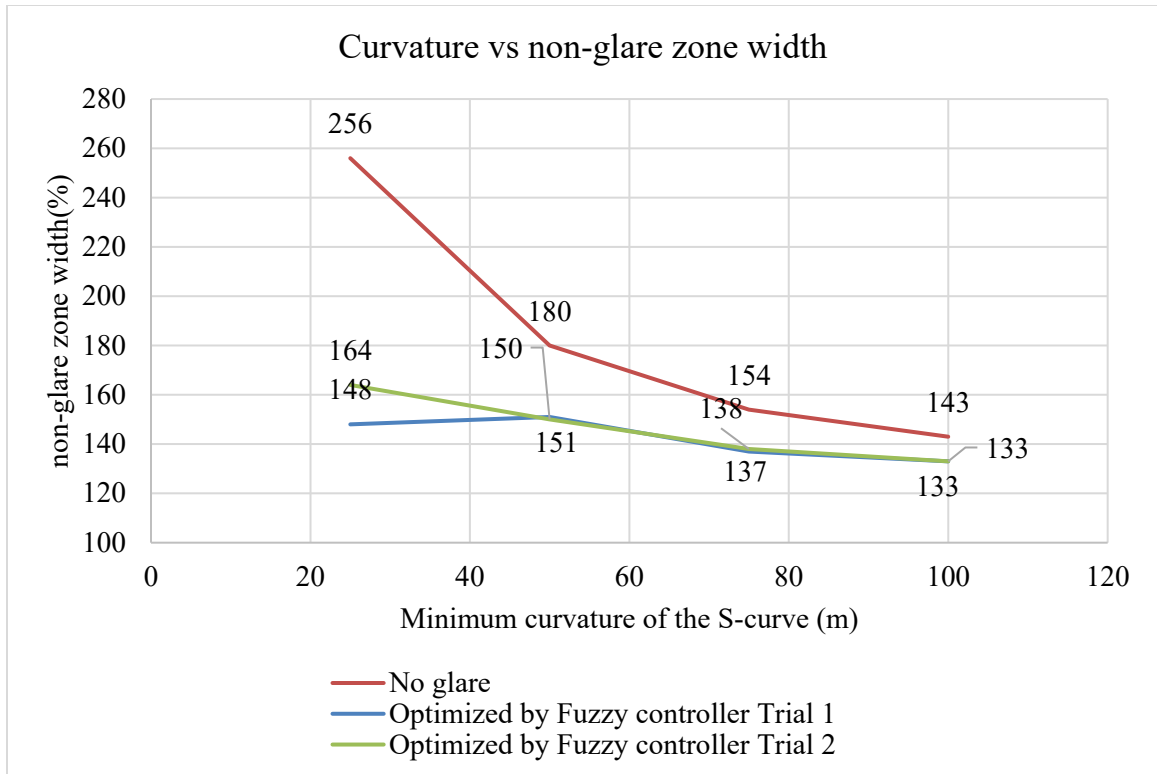


Figure 36. The minimum curvature in the driving scenario vs. best non-glare zone width.

CHAPTER 4

CONCLUSIONS AND FUTURE OPPORTUNITIES

4.1. Conclusions

Adaptive driving beams enhance night driving safety by providing high-beam level road illumination while eliminating the uncomfortable glare that a normal high beam would create for other road users. Due to the limitation of the current vehicle recognition method, indirect glare through side rearview mirrors was observed by the vehicle tailed by an ADB vehicle at sharp corners.

This research focuses on a solution to this issue by providing automotive OEMs with a methodology to develop a design guideline for non-glare zone width adjustment. This research demonstrates a novel methodology to study the trade-off effect between road illumination and glare when tuning the non-glare width in different driving scenarios using a virtual night drive simulator and fuzzy logic control to find the non-glare zone width. Experimenting with a virtual simulator avoids the difficulty and limitations of conventional night drives. The simulation result shows the minimum ADB non-glare zone width to eliminate all glare at S-curves with minimum curvatures at 25m, 50m, 75m, and 100m. The fuzzy logic controller mimics a human test drive to provide feedbacks and balances with the loss of road illumination and the reduction of glare time, converging them to an optimal width. The research also demonstrates fuzzy logic controllers with two basic membership functions, and both of them converge to a similar optimal non-glare zone width in each driving scenario. The pros and cons of solving the glare issue by this methodology are discussed below.

Pros:

- Easy to adopt

The biggest advantage of the methodology for finding the best non-glare zone width with a design guideline is that it does not require the installation of additional hardware and software. The non-glare zone width is one of the parameters of the ADB system that the OEM can adjust when it is received from a supplier. Using the methodology from this research, the design guideline could be developed for all ADB lamps in the fleet. The best non-glare zone width would just be a factory setting.

- Low cost and convenience of research

This research was conducted solely on a virtual night drive simulator. Traditionally, optic experiments on vehicle lighting systems have been conducted in a lighting tunnel, an indoor facility that provides a dark ambient environment, which is usually for conducting static experiments due to the limitation of the facility's size; these experiments have also been conducted on outdoor tracks or proving grounds, in which the testing condition heavily depends on the weather condition. It would also be inconvenient to conduct the outdoor experiment in a high latitude region where, during the summer, sunset occurs later in time. The night drive simulator provides great convenience in conducting dynamic lighting research, as it is not limited by the track size or the ambient influence.

Cons:

- Off-line optimization

Due to the lack of additional inputs, this methodology aims to optimize for a specific driving scenario, while driving scenarios with different curvatures are compromised. An automotive OEM would choose such a curvature based on the region of the vehicles that are being sold. Ideally, the performance of the ADB would be better if an online optimization was applied, meaning the non-glare zone width could dynamically change with the curvature on which the vehicle is travelling.

- The unnecessary sacrifice of road illumination

This methodology enlarges the non-glare zone from both left and right equally, which is also a compromise due to the lack of additional road information. When a vehicle is travelling a corner, the glare only occurs through the inner side rearview mirror. To eliminate such glare, only the non-glare zone needed to enlarge toward the direction of the inner corner, while the other side could remain unchanged. Figure 37 shows an example of the left turn where, ideally, the non-glare zone only needs to enlarge to the left side to minimize the impact on road illumination.

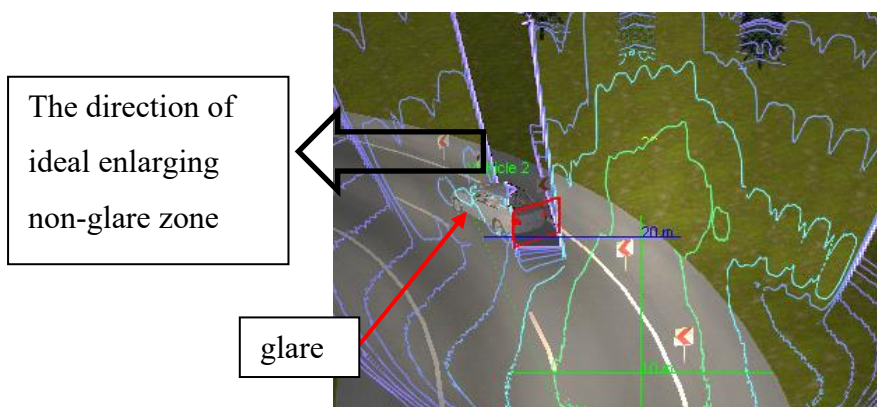


Figure 37. The ideal non-glare zone width enlarging direction for minimizing the effect on road illumination.

The demonstration uses a genetic beam pattern to prove the concept. By replacing the generic beam pattern file with a specific ADB beam pattern, a physical test could be conducted to validate the result from the night drive simulator. The physical test should also collect glare and road illumination feedbacks from the driver, which will be used to select the membership function types and tune the parameters of the fuzzy logic controller.

4.2. Future Opportunities

4.2.1. Physical Test

Considering the difficulty of acquiring an ADB vehicle in North America due to the homologation status of ADB, physical testing of an ADB vehicle was not performed. The correlation study between the physical test and virtual night drive simulation results, however, would be a solid support of this research. Thus, a physical test would be considered for future work.

To perform the correlation study, the simulation should be performed using the beam pattern data of the ADB vehicle that is used in the physical test. Usually, there are two ways to acquire the beam pattern data file; it can be provided by the supplier of the lamp or the lamps from a production vehicle in a lab environment can be scanned. For traditional headlamps, which only have low beam and high beam patterns, it is easy to acquire the beam pattern data file through both methods. With ADB vehicles, however, it may be difficult to obtain the beam pattern data file from suppliers, as it contains technological know-how. Scanning may also be a challenging task. In a production vehicle, the driver can manually switch between low and high beams and the scanning of

those two beam patterns can be carried out accordingly. Since an ADB lamp consists of multiple LEDs that can be automatically switched on and off individually, the overall beam pattern should also consist of the beam patterns of individual LEDs. It is not possible to turn on a single, specific LED in the lamp without accessing the electronic control unit of the lamp, which will very likely require high-level operation privilege authorization. As discussed in Chapter 2, there are two approaches to simulate ADB in the night drive simulator: matrix beam and pixel masking. If the beam pattern data files of individual LEDs are available, the simulation should use the matrix beam approach for better fidelity. If such beam pattern files are not available, the simulation could use the pixel-masking approach with the single beam pattern file of ADB acquired from headlamp scanning.

The physical testing should be performed on a closed curvy track on a dark night, eliminating the ambient influencing factors as much as possible. The test vehicle should be equipped with a lux sensor mounted in the same position in the simulation, for validation purposes. The glare feedback is collected from the stimulus vehicle driver and the road illumination feedback is collected from the ADB vehicle driver. That feedback would help to tune the fuzzy logic controller and improve the optimal result.

4.2.2. Other Optimization Possibilities

Future studies could focus on replacing the fuzzy logic controller used in this research with other optimizers. For example, a neural network could also be used for optimization in this application, if it is given enough data. Such data can be acquired by conducting multiple physical tests and gathering feedback from the test drivers.

4.2.2.1. Sensor Fusion

One possible future development research direction of ADB non-glare zone width is sensor fusion. With additional inputs, the ADB system can better adjust the non-glare zone width accordingly. Here are some ideas for sensor fusion:

4.2.2.2. Steering and Other Vehicle Dynamic Sensors

Using steering input or other vehicle dynamic sensors in this application is not a good idea. The main objective behind having additional sensors is to allow the ADB to predict the maneuver of the stimulus vehicle. Since the stimulus vehicle will be at least two-to-three seconds ahead of the ADB vehicle, using data from onboard vehicle dynamic sensors causes a significant delay before eliminating the glare. Figure 38 is an example of the driving scenario of the S-curve with minimum curvature of 25 m. The graph overlaps the lux reading from the virtual light sensor mounted on the side rearview mirror and the acceleration of the ADB vehicle. The plot shows there is around a one-second delay before the sensors on the ADB vehicle receive signals when the stimulus vehicle experiences glare.

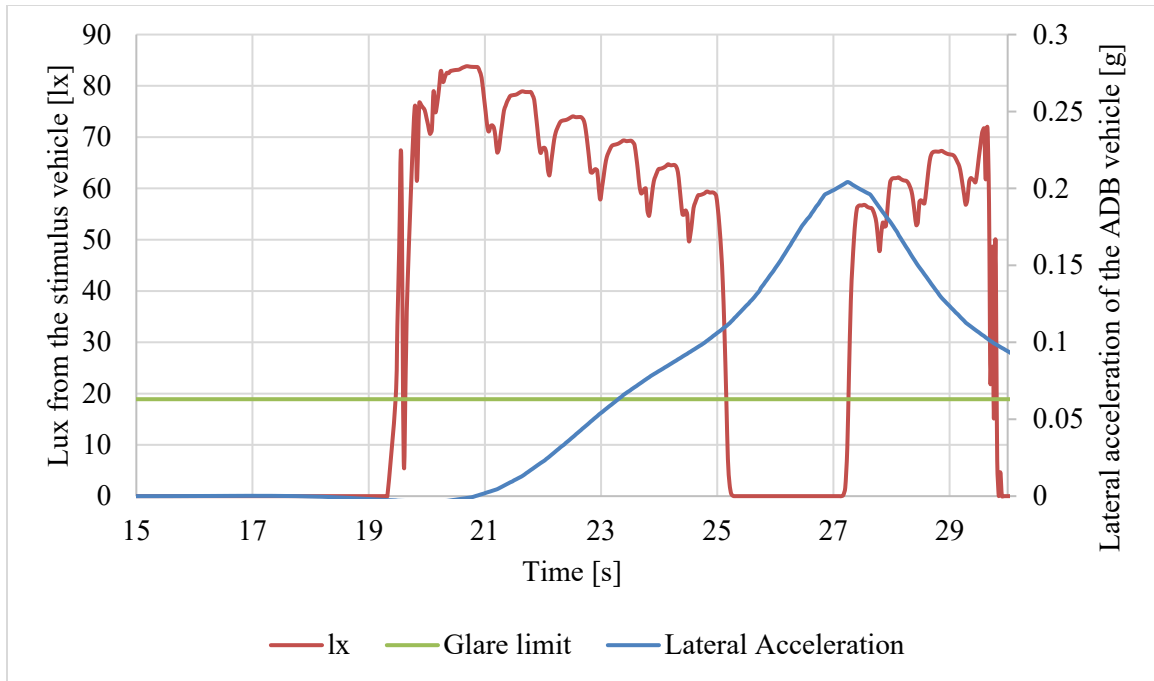


Figure 38. The overlap of the lux reading plot and the lateral acceleration plot, showing the time gap between glare and vehicle dynamic inputs.

4.2.2.3. *Real-Time Optimization: Navigation Information + Distance Sensor*

The navigation system would provide the information about the coming roads, combining it with a distance sensor such as an Adaptive Cruise Control (ACC) radar; this way, the maneuver of the stimulus vehicle can be predicted and the precise width to which the non-glare zone needs to enlarge can be calculated. Besides the challenge of acquiring that information from different systems, it also challenges the computing power of the ADB control unit, as it requires real-time optimization.

4.2.2.4. *Regional Optimization: Navigation Information Only*

Another sensor fusion methodology for ADB non-glare zone optimization that is computationally cheap is combining the non-glare zone optimization design guideline

with the navigation system. Compared to the real-time optimization, the navigation system could provide an average road curvature of a certain area. When the vehicle is travelling in such a region, the non-glare zone width can automatically be tuned to this average curvature's optimized setting according to the guideline. The real-time optimization method requires the navigation system to provide the location information continuously, while the regional optimization method reduces the number of times that the location information is acquired significantly, as it only needs to periodically check in what region the vehicle is travelling.

The future development of ADB would focus on both improving the visual recognition system and the definition of the matrix LED lamp, giving the system more precise control of the non-glare zone to which it projects. Ultimately, night drive safety and comfort will improve as more and more vehicles are equipped with ADB.

REFERENCES/BIBLIOGRAPHY

- [1] Varghese, C. & Shankar, U., “Passenger Vehicle Occupant Fatalities by Day and Night – A Contrast”. (Report No. DOT HS 810 637). Washington, DC: NHTSA’s National Center for Statistics and Analysis., 2007
- [2] Reagan I., Cicchino J., “High Beam Headlights: Self-Reported Frequency of Use, Motivations for Use, and Opinions about Advanced Headlight Technology”, 2016
- [3] Fekety DK, Whetsel SA, Sewall AS, Tyrell RA. “Drivers’ beliefs, habits, and strategies regarding high beam usage”. *Proc. Human Factors and Ergonomics Society 57th Annual Meeting*, pp. 1800-1804. Santa Monica, CA: Human Factors and Ergonomics Society; 2013.
- [4] Sullivan, JM, G Adachi, ML Mefford, and MJ Flannagan. “High-Beam Headlamp Usage on Unlighted Rural Roadways.” *Lighting Research & Technology* 36, no. 1 (March 2004): 59–65.
- [5] American Automobile Association. “Fact Sheet Test Results: Automotive Headlamp Systems.”, 2015
- [6] American Automobile Association, “Comparison of European and U.S. Specification Automotive Headlamp Performance”, 2019.
- [7] Neumann, R., "Adaptive Driving Beam - Visibility Improvement versus Glare," SAE Technical Paper 2014-01-0436, 2014.
- [8] Reagan, I., Brumelow, M. “Perceived Discomfort Glare from an Adaptive Driving Beam Headlight System Compared with Three Low Beam Lighting Configurations”, *Procedia Manufacturing*, Volume 3, 2015, Pages 3214-3221
- [9] United Nations Economic Commission for Europe, “Regulation No 48 of the Economic Commission for Europe of the United Nations (UNECE) — Uniform provisions concerning the approval of vehicles with regard to the installation of lighting and light-signalling devices” 2016

- [10] United Nations Economic Commission for Europe, “Regulation No 123 of the Economic Commission for Europe of the United Nations (UN/ECE) — Uniform provisions concerning the approval of adaptive front-lighting systems (AFS) for motor vehicles” 2019
- [11] Transports Canada. “Motor Vehicle Safety Regulations (C.R.C., c. 1038) - Lighting Systems and Reflective Devices (Standard 108)”. 2018
- [12] National Highway Traffic Safety Administration, “FEDERAL MOTOR VEHICLE SAFETY STANDARDS (Standard No. 108; Lamps, reflective devices, and associated equipment.)”. 2018
- [13] Stricker, T. Toyota Motor North America. Inc, “RE: Petition for Rulemaking to Allow Adaptive High-Beam System into FMVSS No.108”, (Docket No. NHTSA-2013-0004), 2013
- [14] National Highway Traffic Safety Administration (NHTSA), and Department of Transportation (DOT). “Federal Motor Vehicle SAFETY Standards; Lamps, Reflective Devices, and Associated Equipment - A Proposed Rule by the National Highway Traffic Safety Administration on 10/12/2018.” Federal Register, October 12, 2018. <https://www.federalregister.gov/documents/2018/10/12/2018-21853/federal-motor-vehicle-safety-standards-lamps-reflective-devices-and-associated-equipment>. (accessed on 1 September 2021)
- [15] Society of Automotive Engineers, “Adaptive Driving Beam”, SAE International. DOI: 10.4271/J3069_201606, 2013
- [16] “The Newest Lighting System: Products/Technology-Technology of KOITO,” KOITO MANUFACTURING CO., LTD., accessed July 6, 2021, <https://www.koito.co.jp/english/technology/koito/system.html>.
- [17] “Adaptive Driving Beam (ADB) Systems.” OSRAM. Accessed July 6, 2021. https://www.osram.com/os/applications/automotive-applications/exterior_adb_light.jsp.

- [18] “Matrix LED Headlight with Dynamic Laser Spot.” HELLA, Accessed June 22, 2021. <https://www.hella.com/hella-com/en/Headlamps-620.html>.
- [19] “Valeo MatrixBeam - 046834 – 046835 - Technical bulletin” Valeo, Accessed July 6, 2021. <https://www.valeoservice.com/en-com/techassist/technical-bulletin/valeo-matrixbeam-046834-046835>
- [20] LUO, F., & HU, F. “A comprehensive survey of vision based vehicle intelligent front light system”. *International Journal on Smart Sensing and Intelligent Systems*, 7(2), 701-723. doi:10.21307/ijssis-2017-677, 2014
- [21] López, A., Hilgenstock, J., Busse, A., Baldrich, R., Lumbreras, F., & Serrat, J, “Nighttime vehicle detection for intelligent headlight control”, *Advanced Concepts for Intelligent Vision Systems*, Springer Berlin Heidelberg, 2008, pp. 113-124.
- [22] O'Malley, R., Jones, E., Glavin, M., “Rear-lamp vehicle detection and tracking in low-exposure color video for night conditions”, *IEEE Transactions on Intelligent Transportation Systems*, Vol. 11, No.2, June, 2010, pp. 453-462.
- [23] O'Malley, R., Glavin, M., Jones, E., “Vehicle detection at night based on tail-light detection”, 1st international symposium on vehicular computing systems, Trinity College Dublin, 2008.
- [24] O'Malley, R., Glavin, M., Jones, E., “Vision-based detection and tracking of vehicles to the rear with perspective correction in low-light conditions”, *IET Intelligent Transportation Systems*, Vol. 5, Iss. 1, 2011, pp. 1-10.
- [25] Gormer, S., Muller, D., Hold, S., Meuter, M., and Kummer, A., “Vehicle recognition and TTC estimation at night based on spotlight pairing”, Proceedings of the 12th International IEEE Conference on Intelligent Transportation Systems, St.Louis, MO, USA, 3-7 October 2009, pp. 196-201.
- [26] Tehrani, H., Kawano, T., & Mita, S. “Car detection at night using latent filters”. 2014 IEEE Intelligent Vehicles Symposium Proceedings. 2014, doi:10.1109/ivs.2014.6856518

- [27] Pengkang Zeng, JinTao Zhu, GuoHeng Huang, and LiangLun Cheng. "Color Recognition of Vehicle Based on Low Light Enhancement and Pixel-wise Contextual Attention". In 2020 2nd Symposium on Signal Processing Systems (SSPS 2020). Association for Computing Machinery, New York, NY, USA, 13–17. 2020. DOI:<https://doi.org/10.1145/3421515.3421527>
- [28] B. Balci, A. Elihos, M. Turan, B. Alkan and Y. Artan, "Front-View Vehicle Make and Model Recognition on Night-Time NIR Camera Images," 2019 16th IEEE International Conference on Advanced Video and Signal Based Surveillance (AVSS), 2019, pp. 1-6, doi: 10.1109/AVSS.2019.8909880
- [29] Götz, M., Lee, H. M., Han, S. Y., & Sung, J. Y. "Sensor fusion for improvement of Adaptive high beam". *ATZ Worldwide*, 121(10), 2019, 42-45. doi:10.1007/s38311-019-0109-0
- [30] Gao, Z., & Li, Y., "Control algorithm of Adaptive Front-lighting system based on Driver preview behavior". Proceedings of 2013 2nd International Conference on Measurement, Information and Control., 2013, doi:10.1109/mic.2013.6758218
- [31] Bradai, B., et al. "Predictive navigation-based virtual sensor for enhanced lighting." International Symposium on Automotive Lighting (ISAL). Vol. 26. 2007
- [32] Synopsys. *LucidDrive Manual - LucidDrive Night Drive Simulation*, 2018, Available: <https://www.synopsys.com/support.html>
- [33] Technical Committee ISO/TC29/SC9. "Road vehicles – Vehicle dynamics and road-holding ability –Vocabulary"
- [34] Synopsys. *RoadEditor Manual - LucidDrive Night Drive Simulation*, 2018, Available: <https://www.synopsys.com/support.html>
- [35] American Association of State Highway and Transportation Officials. *A policy on geometric design of highways and streets*, Washington, D.C., 2001

- [36] Mazzae, E. N., Baldwin, G. H. S., Andrella, A., & Smith, L. A. "Adaptive driving beam headlighting system glare assessment". (Report No. DOT HS 812 174). Washington, DC: National Highway Traffic Safety Administration., 2015
- [37] National Safety Council. Following Distance - Three-second following distance. In *Defensive Driving Courses - The DDC Instructor And Administrative Reference Guide*, United States, 2005
- [38] Lotfi, Zadeh. "Fuzzy sets" *Information and control* 8.3. 1965: 338-353.
[https://doi.org/10.1016/S0019-9958\(65\)90241-X](https://doi.org/10.1016/S0019-9958(65)90241-X)
- [39] MathWorks. Fuzzy Logic Toolbox: User's Guide. Accessed September 4, 2021.
<https://ww2.mathworks.cn/help/fuzzy/index.html>

VITA AUCTORIS

NAME: Yihong Chen

PLACE OF BIRTH: Guangzhou, Guangdong, China

YEAR OF BIRTH: 1994

EDUCATION: Guangzhou No.16 Middle School, Guangzhou, China, 2013

University of Windsor, B.Sc., Windsor, ON, 2019

University of Windsor, M.ASc., Windsor, ON, 2021

Politecnico di Torino, M.Sc., Torino, Italy, 2021